1

Transient-State Kinetic Analysis of Enzyme Reaction Pathways

KENNETH A. JOHNSON

Department of Molecular and Cell Biology
The Pennsylvania State University
University Park, Pennsylvania 16802

I. Introduction

Two fundamental questions underscore studies in enzymology and can be addressed by proper kinetic analysis: (1) elucidation of the enzymic reaction pathway to identify reaction intermediates and to specify the steps that limit the rate of turnover and (2) quantitative evaluation of the use of binding energy for enzyme specificity and catalysis. In this chapter, I will describe transient-state kinetic methods and analyses that allow the direct measurement of rate and equilibrium constants governing individual steps of an enzymic reaction pathway. Emphasis will be placed on the application of two rapid mixing methods, stopped-flow and chemical-quench-flow. In the past, two factors have limited the application of transient kinetic methods to enzymology: the amounts of enzyme required to perform such studies and the complexity of the equations describing the time dependence of transient reactions. Substantial improvements in the instrumentation (*1*) and the availability of cloned, overexpressed enzymes have largely eliminated the concerns over quantities of enzyme. The complexities of data analysis have been overcome by advances in computational methods to analyze reaction time courses by numerical integration (*2*, *3*).

The last time this topic was reviewed in "The Enzymes" (*4*), the chapter dealt largely with the solution of differential equations necessary to interpret transient kinetic data, and only a small section described computational methods used to fit data by numerical integration. To a great extent, work was dependent on the simplification of reaction pathways to allow explicit solution of the rate equations describing the time dependence of each species in the reaction sequence. Moreover, the need to fit data to an explicit solution greatly restricted the design of experiments. Equilibrium perturbation methods were preferred, in large part, because of the ability to linearize differential equations describing systems near equilibrium. All of that has changed due to the recent advances in computational methods. One is no longer restricted to simplified reaction schemes or tied to tedious analysis of differential equations in seeking solutions of rate equations. Experiments can now be performed without restrictions for the starting conditions of the experiment dictated by the easy solution of the rate equations, and the results can be analyzed by the fitting of the data directly to a kinetic scheme. For these reasons, we are now free to focus in this chapter on the logical design of experiments and attempt to develop an intuitive understanding of the

kinetics of enzyme reactions. I will refer to the equations describing the time dependence of reactions only to help in the development of an understanding of multiple-step reaction sequences and in the quantitative analysis of reaction rates in simplified cases. Reference to the literature will be selective rather than exhaustive, drawing on a few examples wherein transient kinetic methods have afforded a quantitatively complete analysis of each step in the reaction sequence to illustrate the conceptual basis for these studies.

II. Rationale for Transient Kinetic Analysis

A. Limitations of Steady-State Kinetics

The kinetic analysis of an enzyme mechanism often begins by analysis in the steady state; therefore, we first consider the conclusions that can be derived by steady-state analysis and examine how this information is used to design experiments to explore the enzyme reaction kinetics in the transient phase. It has often been stated that steady-state kinetic analysis cannot prove a reaction pathway, it can only eliminate alternate models from consideration (*5*). This is true because the data obtained in the steady state provide only indirect information to define the pathway. Because the steady-state parameters, k_{cat} and K_m, are complex functions of all of the reactions occurring at the enzyme surface, individual reaction steps are buried within these terms and cannot be resolved. These limitations are overcome by examination of the reaction pathway by transient-state kinetic methods, wherein the enzyme is examined as a stoichiometric reactant, allowing individual steps in a pathway to be established by direct measurement. This is not to say that steady-state kinetic analysis is without merit; rather, steady-state and transient-state kinetic studies complement one another and analysis in the steady state should be a prelude to the proper design and interpretation of experiments using transient-state kinetic methods. Two excellent chapters on steady-state methods have appeared in this series (*6*, *7*) and they are highly recommended.

For practitioners of steady-state kinetics, the "kinetic mechanism"of an enzyme is defined by specifying the order of addition of substrates and the order of release of products. This analysis defines which reactants are present at the active site of the enzyme during the chemical reaction, for example, by distinguishing Ping-Pong versus sequential mechanisms. However, no information is available to define the steps in the reaction involving enzyme-bound species or to identify the rate-limiting step. Enzyme mutations, pH variation, or alternate substrates can slow the rate of a chemical reaction so that it becomes rate limiting in the steady state, and the examination of isotope effects can probe the extent to which chemistry is rate limiting (*8*, *8a*, *8b*). Direct measurements of reactions at the enzyme active site are required in order to establish the kinetic and thermody-

namic bases for enzymic specificity and efficiency. We must redefine what constitutes proof of an enzyme reaction mechanism to include direct measurement of individual reactions occurring at the enzyme active site at physiological pH and with the natural substrates.

B. Meaning of K_m and k_{cat}

The two kinetic constants, K_m and k_{cat}, are most often misinterpreted as the substrate dissociation constant and the rate of the chemical reaction, respectively. However, this is not always the case, and K_m can be greater than, less than, or equal to the true substrate dissociation constant, K_d. The steady-state kinetic parameters only provide information sufficient to describe a minimal kinetic scheme. In terms of measurable steady-state parameters, a reaction sequence must be reduced to a minimal mechanism (Scheme I),

$$E + S \underset{k_{-1}}{\overset{k_1}{\rightleftharpoons}} E{\cdot}S \xrightarrow{k_2} E + P$$

Scheme I

where the steady-state parameters are defined by

$$k_{cat} = k_2; \qquad K_m = (k_2 + k_{-1})/k_1 \tag{1}$$

This simplified model can be understood as resulting from the kinetic collapse of a more realistic mechanism (Scheme II).

$$E + S \underset{k_{-1}}{\overset{k_1}{\rightleftharpoons}} E{\cdot}S \underset{k_{-2}}{\overset{k_2}{\rightleftharpoons}} E{\cdot}P \xrightarrow{k_3} E + P$$

Scheme II

The minimal complete model shown in Scheme II leads to the following steady-state parameters:

$$k_{cat} = \frac{k_2k_3}{k_2 + k_{-2} + k_3}$$
$$K_m = \frac{k_2k_3 + k_{-1}k_{-2} + k_{-1}k_3}{k_1(k_2 + k_{-2} + k_3)} \tag{2}$$

A reaction pathway containing a single intermediate as shown later in Scheme III (p. 6) leads to even more complex expressions for k_{cat} and K_m:

$$k_{cat} = \frac{k_2k_3k_4}{(k_2 + k_{-2})(k_{-3} + k_4) + k_2k_3 + k_3k_4}$$
$$K_m = \frac{k_{-1}(k_{-2}(k_{-3} + k_4) + k_3k_4) + k_2k_3k_4}{k_1((k_2 + k_{-2})(k_{-3} + k_4) + k_2k_3 + k_3k_4)} \tag{3}$$

Thus k_{cat} and K_m are a function of all the rate constants in the pathway and any simplifying assumptions concerning individual rate constants are likely to be inaccurate. Moreover, the three reaction pathways shown in Schemes I and II, and III are indistinguishable by steady-state methods. Although product inhibition patterns provide evidence for the E·P state, individual kinetic constants cannot be resolved. Schemes II and III reduce to Scheme I under the conditions where $k_3, k_4 \gg k_2$. Steady-state kinetics cannot resolve the three reaction mechanisms because the form of the equation for steady-state kinetics is identical for each mechanism (v = rate):

$$v/[E_0] = \frac{k_{cat}[S]}{K_m + [S]} \tag{4}$$

Only the complexity of the expressions for k_{cat} and K_m differ.

The two fundamental-steady state kinetic constants are the terms k_{cat}, the maximum rate of product formation at saturating substrate, and k_{cat}/K_m, the *apparent* second-order rate constant for *productive* substrate binding. The value of K_m should only be considered as a ratio of the maximum rate of decomposition of the enzyme–substrate complex divided by the *apparent* rate of substrate binding (*6*). This understanding more accurately reflects the magnitude of K_m as representing the concentration of substrate at which the rate of substrate binding during the steady-state conversion of substrate to product equals the sum of the rates of substrate and product release. The two steady-state kinetic constants provide lower limits for the intrinsic rate constants that govern an enzymic reaction. The value of k_{cat}/K_m represents a lower limit for the rate of substrate binding, and k_{cat} sets a lower limit on the magnitude of any first-order rate constant following the binding of substrate and proceeding to the release of products.

With this perspective, one can summarize the three things learned by steady-state kinetic analysis as follows:

1. The order of binding of substrates and release of products serves to define the reactants present at the active site during catalysis; it does not establish the *kinetically preferred* order of substrate addition and product release or allow conclusions pertaining to the events occurring between substrate binding and product release.

2. The value of k_{cat} sets a lower limit on each of the first-order rate constants governing the conversion of substrate to product following the initial collision of substrate with enzyme. These include conformational changes in the enzyme–substrate complex, chemical reactions (including the formation and breakdown of intermediates), and conformational changes that limit the rate of product release.

3. The value of k_{cat}/K_m defines the apparent second-order rate constant for substrate binding and sets a lower limit on the true second-order rate constant for substrate binding. The term k_{cat}/K_m is less than the true rate constant by a

factor defined by the kinetic partitioning of the E·S complex to dissociate or go forward in the reaction. The magnitude of k_{cat}/K_m is used to quantitate enzyme specificity, but it cannot be used to establish the kinetic and thermodynamic basis for enzyme specificity, a goal that can only be achieved by analysis of individual reaction steps.

C. Goals of Complete Kinetic Analysis

To begin, we will base our analysis on a theoretical enzyme reaction pathway occurring by the sequence in Scheme III,

$$E + S \underset{k_{-1}}{\overset{k_1}{\rightleftharpoons}} E{\cdot}S \underset{k_{-2}}{\overset{k_2}{\rightleftharpoons}} E{\cdot}X \underset{k_{-3}}{\overset{k_3}{\rightleftharpoons}} E{\cdot}P \underset{k_{-4}}{\overset{k_4}{\rightleftharpoons}} E + P$$

Scheme III

where E·X represents an enzyme intermediate that can be defined as a distinct chemical species or a unique kinetically significant conformational state such as one formed by a change in structure of the E·S complex preceding the chemical reaction. Throughout this review, I will use a nomenclature in which k_n and k_{-n} represent the rate constants in the forward and reverse directions, respectively, for the nth step in the reaction sequence and K_n represents the equilibrium constant written in the forward direction.

Enzyme reaction mechanisms involving multiple substrates can be understood intuitively and addressed experimentally in terms of the one-substrate case by examining partial reactions along the sequence, or by considering the kinetics at saturating concentrations of the cosubstrates. Even with this simplification, as we will describe below, all data can and should be fit to the complete reaction pathway involving all substrates, products, and intermediates. Computer simulation based on the complete reaction sequence ensures that the data can be quantitatively understood in terms of the reaction sequence, with no simplifying assumptions. The extent to which all of the rate constants in the pathway are constrained during the fitting process by the experimental evidence is dependent on deriving the minimal mechanism.

According to the reaction sequence defined in Scheme III, the goal of a complete kinetic analysis is to provide estimates for each of the eight rate constants and four equilibrium constants. Measurement of the equilibrium constants can often provide a means to estimate individual rate constants that cannot be measured directly; moreover, redundancy in measurements of rate and equilibrium constants provide a check for internal consistency. In the process of measuring each rate constant, the identities and kinetic competence of potential intermediates will be established, and the resulting free energy profile for the reaction pathway will help to define the relationship between binding energy and catalytic efficiency. This information then serves as a background for analysis of proteins altered by site-directed mutagenesis to examine the roles of individual amino

acids or groups of amino acids in substrate binding and transition-state stabilization (*8*). Alternatively, measurement of the changes in intrinsic rate constants occurring with altered substrates, mutated by chemical synthesis, establishes the kinetic and thermodynamic bases for enzyme specificity. Thus, whether one alters the substrates or the enzyme, it is necessary to assess the effects of such alterations on catalysis by quantitation of the changes in individual steps in the reaction sequence. These thermodynamic terms can then be related to the structural alterations to define the ways in which binding energy is used to carry out selectively catalysis of desired reactions.

The effect of mutations on steady-state parameters is rather boring in most cases: k_{cat} decreases and K_m increases. However, transient-state kinetic analysis has revealed many interesting properties of mutated enzymes (*8*, *9*). For example, in studies on tyrosyl-tRNA synthetase (EC 6.1.1.1, tyrosine-tRNA ligase), Fersht and co-workers have quantitated changes in ground-state and transition-state binding energy by measurement of the binding constants and rate of the chemical reaction in single-turnover experiments for mutations in residues contacting the substrates (*9*). In recent work on DNA polymerase, we have established the kinetic and thermodynamic bases for fidelity by single-turnover experiments to measure changes in binding energy, rates of substrate binding, and changes in rate of chemical reaction occurring on substitution of incorrect nucleoside triphosphates (*10–12*). Neither of these goals could have been achieved without direct measurement of events occurring at the enzyme active site by transient kinetic methods.

D. Rationale for Designing Transient Kinetic Experiments

Although steady-state kinetic methods cannot establish the complete enzyme reaction mechanism, they do provide the basis for designing the more direct experiments to establish the reaction sequence. The magnitude of k_{cat} will establish the time over which a single enzyme turnover must be examined; for example, a reaction occurring at 60 sec^{-1} will complete a single turnover in approximately 70 msec (six half-lives). The term k_{cat}/K_m allows calculation of the concentration of substrate (or enzyme if in excess over substrate) that is required to saturate the rate of substrate binding relative to the rate of the chemical reaction or product release. In addition, the steady-state kinetic parameters define the properties of the enzyme under multiple turnovers, and one must make sure that the kinetic properties measured in the first turnover mimic the steady-state kinetic parameters. Thus, steady-state and transient-state kinetic methods complement one another and both need to be applied to solve an enzyme reaction pathway.

Analysis of steady-state kinetics can also reveal those cases in which rapid mixing methods are likely to fail or at least be more difficult to perform. For example, because one must examine a single enzyme turnover, enzymes with exceedingly high k_{cat} values (greater than 1000 sec^{-1}) are not amenable to rapid

mixing methods unless the rates are slowed by working at reduced temperatures. Faster rates of reaction can be measured by temperature jump or pressure jump methods (*13*, *14*), but, as we will describe later, mechanistic information is obtained by examining the concentration dependence of the reaction and this is often difficult to obtain by equilibrium perturbation methods. For these reasons, we will restrict our attention to two rapid mixing methods, stopped-flow and chemical-quench-flow, for measurement of the rates of enzyme-catalyzed reactions.

A second limitation of the single-turnover or presteady-state burst experiment arises with those enzymes that exhibit a high K_m relative to the accessible concentrations of enzyme. For example, in studies of ATPases, the background of inorganic phosphate is difficult to get much below 1% of the total ATP. Thus, if the enzyme requires 1m*M* ATP to saturate the enzyme–substrate complex, it is necessary to use at least 10 μM enzyme to have a signal as large as the background in attempting to measure the rate of hydrolysis at the active site. When the separation of products from the substrates is easier to perform, such as in studies on DNA polymerase, one can accurately quantitate the formation of 100 n*M* product in the presence of 100 μM substrate (*10*). In ideal cases, experiments can be performed with enzyme in excess over substrate and thereby examine 100% conversion of substrate to product in a single enzyme turnover with a high degree of sensitivity in looking for enzyme intermediates (*3*, *15*).

Perhaps the most difficult aspect of learning transient-state kinetic methods is that it is not possible to lay down a prescribed set of experiments to be performed in a given sequence to solve any mechanism. Rather, the sequence of experiments will be dictated by the details of the enzyme pathway, the relative rates of sequential steps, and the availability of signals for measurement of rates of reaction. The latter constraint applies mainly to stopped-flow methods, and less so for chemical-quench-flow methods provided that radiolabeled substrates can be synthesized. Therefore, I will describe the kinetic methods used to establish an enzyme reaction mechanism with emphasis on the direct measurement of the chemical reactions by rapid quenching methods. Stopped-flow methods are useful in instances in which optical signals provide an easy means to measure the rates of individual steps of the reaction.

A reasonable sequence of experiments toward establishing the mechanism of an enzyme-catalyzed reaction can be put forth. In suggesting the order in which experiments should be carried out, the emphasis is in providing a logical progression of information wherein each experiment can be designed based on the quantitative information provided by the previous results. In general, the analysis begins at the ends of the pathway and works toward the center. The following protocol provides an outline for the experiments presented in the order that is most logical, although not all measurements will be possible in all cases and the prescribed order is not absolute.

1. Use steady-state kinetic methods to determine k_{cat} and K_m for the reaction, in each direction if it is reversible, and to determine the sequence of addition of substrates and release of products. In some cases the orders of substrate binding or product release may not be easy to determine unambiguously by steady-state methods, and so further tests by transient kinetic methods may be necessary.
2. Perform equilibrium measurements to establish the overall free energy of the reaction in solution, and, if possible, the internal equilibrium constants for reactions occurring at the active site. In addition, it is often possible to measure the equilibrium dissociation constants for the binding of any substrates that, by themselves, will bind and not react, such as the first substrate to bind in a multiple-substrate mechanism.
3. Measure the rates of substrate binding and dissociation by stopped-flow methods or by substrate trapping methods. This is an optional step in that although information on binding rates can be useful, it is not essential for the design of subsequent experiments.
4. Look for a presteady-state burst of product formation by chemical-quench-flow methods to determine if a step after chemistry is at least partially rate limiting and to then measure the rate and equilibrium constant for the chemistry step.
5. Perform single-turnover experiments with enzyme in excess of substrate to examine more closely the conversion of substrates to products at the active site of the enzyme and to look for intermediates.
6. Put all of the kinetic and equilibrium data together into a single, complete model for the reaction sequence, quantitatively accounting for every experimental result by the complete reaction pathway. Computer simulation can be used to establish that all experimental results can be understood quantitatively in terms of a single mechanism.

It should be noted that a complete, quantitative kinetic analysis can provide the framework with which an investigation proceeds to completion, with other direct, structural methods applied to the problem as they are suggested by the kinetic data. For example, observation and kinetic characterization of an intermediate will define the conditions required to isolate the intermediate and prove its structure by other methods (*15*, *16*). The structural and kinetic methods complement one another and neither can be interpreted rigorously without the other (*16*, *17*).

It should become apparent that when one begins a study, the information required to properly design the experiments is not entirely in hand. The approach must be an iterative one in which initial estimates provide the means to make some initial measurements, and as the information on the kinetics of the reaction is refined, the measurements can be repeated to approach a final convergence of the solution of the mechanism. Such an approach was successful in defining all 12 rate constants in the reaction catalyzed by 5-enolpyruvoylshikimate-3-

phosphate (EPSP) synthase, including identification, isolation, and kinetic characterization of an intermediate formed at the active site (*15*, *16*).

This outline describing the logical progression of experiments will be followed for the remainder of this chapter. We begin with equilibrium measurements.

III. Experimental Methods for Complete Kinetic Analysis

A. Measurement of Equilibrium Constants Governing Catalysis

For a simple enzyme-catalyzed reaction (Scheme IV) it is often possible to measure each of the equilibrium constants, K_1, K_2, K_3, and $K_{net} = K_1K_2K_3$.

$$E + A \underset{k_{-1}}{\overset{k_1}{\rightleftharpoons}} E{\cdot}A \underset{k_{-2}}{\overset{k_2}{\rightleftharpoons}} E{\cdot}P \underset{k_{-3}}{\overset{k_3}{\rightleftharpoons}} E + P$$

SCHEME IV

Because of the conversion of substrate to product and the reverse, it is obviously not possible to measure directly by equilibrium methods the binding constants for substrate and product. However, the binding constants can be estimated from the ratio of the binding and dissociation rates. The methods, interpretation, and limits of such measurements will be described below.

1. *Overall Equilibrium*

The net overall equilibrium constant for the reaction in solution (K_{net}) and the internal equilibrium constant for reaction at the active site (K_{int}) can be measured most easily using radiolabeled substrates. Thus the problem becomes one of separating substrate and product chromatographically and then quantitating the ratio of K_{net} = [P]/[S] following incubation of the substrate with a trace of enzyme for a time sufficient for the reaction to come to equilibrium. The equilibration time can be estimated from the magnitude of k_{cat}/K_m in the forward and reverse reactions. If the substrate and product concentrations are below their K_m values, then the rate of approach to equilibrium can be approximated by

$$k_{obs} \simeq (k_{cat}/K_m)^{for}[E] + (k_{cat}/K_m)^{rev}[E] \qquad (5)$$

The reaction will be 98% complete after six half-lives: $t_{1/2} = \ln 2/k_{obs}$. Alternatively, if the starting concentration of substrate, $[S]_0$, is greater than the K_m, then the time required to approach equilibrium can be approximated from $\Delta t = [S]_0/k_{cat}[E]$. Measurement of the product/substrate ratio at the time calculated and at twice the time will ensure the attainment of equilibrium.

The concentration of enzyme added should be dictated on the one hand by the desire to minimize the time required to reach equilibrium relative to the stability of the reactants and products, and on the other hand by the requirement that the concentration of enzyme be negligible relative to the concentration of the least abundant reactant at equilibrium. Here the need for caution is to ensure that the concentration of substrate or product measured is due to that in solution and not that bound to the enzyme.

2. *Internal Equilibrium*

The internal equilibrium constant can be measured after finding conditions under which *all* of the substrate and product will be bound to the enzyme. This is done by working at concentrations of enzyme in 5- or 10-fold excess of the dissociation constants for each substrate. Accordingly, the ratio of [P]/[S] measured will reflect the ratio of $[E{\cdot}P]/[E{\cdot}S] = K_{int}$. The time required for the reaction to come to equilibrium can be approximated from the relationship $k_{obs} \geq k_{cat}^{for} + k_{cat}^{rev}$ to provide a minimum estimate of the rate of reaction at the active site. Usually the time calculated will be in the millisecond domain, but incubation for 5 sec is more convenient for manual mixing and usually no side products are formed on this time scale. Although in some cases it may be difficult to obtain concentrations of enzyme in excess of the dissociation constants for the substrates and products, the quantitation of the product/substrate ratio can be done quite accurately thanks to the fundamental property of enzyme catalysis that leads to an internal equilibrium constant close to unity for most enzymes (*18–20*).

Similar methods can be applied to enzymes catalyzing the reactions of two or more substrates, although there are actually some advantages afforded by this seemingly greater complexity. For example, consider the Bi Bi ordered reaction sequence (Scheme V).

$$E + A + B \underset{k_{-1}}{\overset{k_1}{\rightleftharpoons}} E{\cdot}A + B \underset{k_{-2}}{\overset{k_2}{\rightleftharpoons}} E{\cdot}A{\cdot}B \underset{k_{-3}}{\overset{k_3}{\rightleftharpoons}} E{\cdot}P{\cdot}Q \underset{k_{-4}}{\overset{k_4}{\rightleftharpoons}} E{\cdot}Q \underset{k_{-5}}{\overset{k_5}{\rightleftharpoons}} E + Q + P$$

SCHEME V

First it should be noted that the equilibrium constants for binding A and Q can be measured by standard equilibrium methods, thus the problem reduces to the central reactions that parallel the simple one-substrate reaction described above. Moreover, one can measure the overall and internal equilibria by placing radiolabel in the substrate A and quantitating its conversion to product Q. For the external equilibrium measurement, the ratio of unlabeled [P]/[B] can be altered to bring the ratio of labeled [Q]/[A] close to unity to allow more accurate measurement (*3*), allowing the overall equilibrium constant to be calculated from K_{net} = [P][Q]/[A][B].

The internal equilibrium is also more easily measured by taking advantage of the mass action afforded by working at high concentrations of unlabeled B and P to force the reaction toward the central complexes. Thus by working with enzyme in excess of the limiting radiolabeled substrate, A, and using a high

concentration of B to drive the reaction forward and a high concentration of P to drive the reaction toward the reverse, the internal equilibrium constant can be measured directly from the ratio of radiolabeled A and Q: [Q*]/[A*] = [E·P·Q]/[E·A·B]. In the case of EPSP synthase, the internal equilibrium measurements afforded equilibrium constants both for the formation of an intermediate from substrates and for its breakdown to products (*3*, *16*).

It should also be noted that a multisubstrate enzyme also allows the application of substrate trapping methods to estimate the rates of dissociation of the first substrate to bind to the enzyme. These methods will be described in Section IV,F,2.

The importance of equilibrium measurements cannot be overly stressed. They provide true thermodynamic constants to evaluate the role of substrate binding in catalysis, they provide the background with which kinetic experiments can be properly designed and interpreted to establish the pathway of catalysis, and they provide additional constraints to be used in the fitting of kinetic data.

B. Rapid Mixing Transient Kinetic Methods

I will describe only briefly the instrumental methods used to collect data and I will limit this discussion to rapid mixing methods (stopped-flow and chemical-quench-flow) because these methods allow measurement of the concentration dependence of reaction rates, providing important mechanistic information (*1*). Methods of data fitting will be presented at the end of the chapter.

1. *Stopped-Flow Methods*

Stopped-flow methods are useful whenever there is an optical signal for the reaction of interest. Absorbance changes have been useful in several reactions, including enzymes containing a reactive heme (*21*, *22*) or pyridoxal phosphate (*23–26*), or reactions involving NADH (*27*). Absorbance changes are relatively easy to measure instrumentally, but they depend on changes in extinction coefficient between substrate and product, and the absorbance by the substrate free in solution can limit the sensitivity of the method in attempting to detect changes occurring at the enzyme active site when substrate is in large excess over enzyme.

A stopped-flow experiment is quite simple in principle. The apparatus allows the rapid mixing of two or more solutions, which then flow into an observation cell while the previous contents are flushed and replaced with freshly mixed reactants (Fig. 1). A stop syringe is used to limit the volume of solution expended with each measurement and also serves to abruptly stop the flow and to trigger simultaneously a computer to start data collection. Thus, if one were to watch from the point of view of the photodetector, one would first see the solution flow into the observation cell and then abruptly stop. The reaction is followed as the solution ages after the flow stops. The time resolution of the method

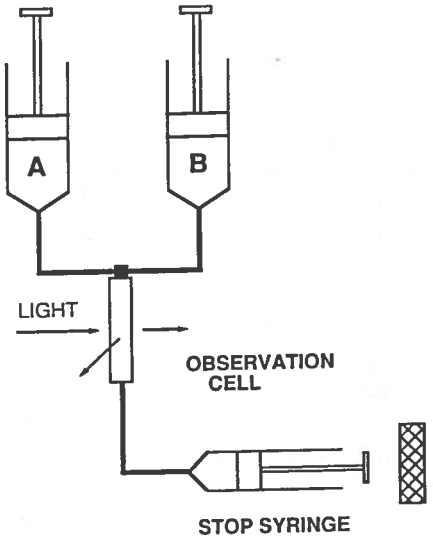

Fig. 1. Schematic of stopped-flow apparatus.

is limited by the time required for the reactants to flow from the point of mixing to the point of observation; this "dead time" is typically on the order of 1–4 msec, depending on the apparatus. Thus, half of the signal is lost at rates of 175 sec^{-1} (4 msec dead time) to 700 sec^{-1} (1 msec dead time). The ability to measure a reaction is limited by the signal-to-noise ratio and so rates in excess of 1000 sec^{-1} have been measured (*27*) in cases in which the signal was particularly good, even though the measurement was based upon less than half of the original amplitude.

Fluorescence methods provide several advantages over absorbance due to the greater signal-to-noise ratio resulting from the lower background. For example, there are numerous cases in which protein fluorescence methods have allowed measurements of the rates of changes in conformation of the enzyme during substrate binding and catalysis (*28*, *29*). In other cases the use of a fluorescent substrate or product (natural or synthetic) has provided accurate measurement of reactions occurring at the active site (*30*, *30a*). For example, the use of fluorescence energy transfer from the protein to bound NADH has afforded a signal measuring the conversion of NADH to NAD^+ at the enzyme active site (*27*). The major limitation to fluorescence methods is that relatively intense light sources are required (in comparison to absorbance methods) and particular attention must be made to achieve efficient recovery of the light emitted from the sample.

The measurement of signal amplitude is often overlooked in studies of reaction rates; however, important information is contained in the amplitude. For ex-

ample, the absolute amplitude of formation of a transient intermediate is essential to resolve the kinetics of its formation and decay. In other cases, evidence for a fast phase of a reaction can be obtained by loss of signal amplitude beyond that expected from the observable rate of reaction and the known dead time of the instrument. For example, in studies on the myosin ATPase, evidence for a fast binding reaction was obtained by noting the loss of 40% of the protein fluorescence signal amplitude at a rate of 125 sec^{-1} (*28*). From the dead time of the instrument, equal to 1.5 msec, one would expect the loss of only 17% of the signal, calculated from $A/A_0 = e^{-kt_d}$, where t_d is the dead time. The greater loss in signal was correlated with the ATP binding rate measured by dissociation of the actomyosin complex, approaching a maximum rate of ~2000 sec^{-1}. The fast phase was confirmed by direct observation at lower temperature.

In order to observe a reaction in a stopped-flow experiment, data must be collected over the proper time window. Because the method spans some five orders of magnitude in time, it is easy to miss a reaction because it was either too fast or too slow to be observed on the time scale selected. The rule is to observe the reaction over six half-lives. An iterative method should be applied. Initial estimates of the rate are used to select the time over which to examine the reaction; the measured rate is then used to adjust the time of data collection, eventually converging on the optimal time according to the rate of the reaction.

2. *Chemical-Quench-Flow Methods*

The most serious limitation of stopped-flow methods is that one does not always have an optical signal for the reaction of interest and the optical signals cannot be interpreted rigorously if the extinction coefficients of intermediates or products are not known. For example, an enzyme intermediate may have an unknown extinction coefficient, and without an absolute measurement of concentration of the intermediate, one cannot obtain a unique solution to its rate of formation and decay (see below). For these reasons, a direct measurement of the conversion of substrate to product is required. Chemical-quench-flow methods allow such direct measurement of the chemistry of enzyme-catalyzed reactions and can be performed for nearly any reaction. One must recognize that these experiments are based on examining the enzyme as a stoichiometric reactant such that the concentration of enzyme required will depend upon the kinetics of the reaction and the sensitivity of the methods for detection of intermediates or products. Nonetheless, quench-flow experiments can be performed using as little as 20 μl of solution and a complete enzyme pathway can be solved using only 5–10 mg of enzyme.

The chemical-quench-flow apparatus allows the mixing of two reactants, followed, after a specified time interval, by mixing with a quenching agent, usually acid or base, to denature the enzyme and liberate any enzyme-bound intermediates or products. A simple quench-flow apparatus is illustrated schematically in Fig. 2.

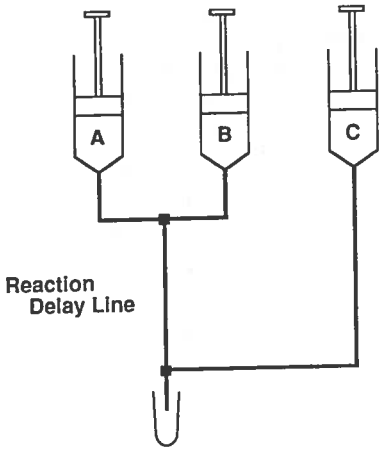

FIG. 2. Standard quench-flow apparatus.

A precisely controlled motor is used to drive syringes containing enzyme (syringe A), substrate (syringe B), and quench solution (syringe Q). Enzyme and substrate are first mixed and the reaction proceeds as the reaction mixture flows through a reaction loop of defined length. Reaction is terminated when the enzyme–substrate solution is mixed with quenching solution. The time of reaction is determined by the volume of the reaction loop between the two points of mixing and the rate of flow. In practice, the reaction time is varied by changing the length of tubing in the reaction loop and, to a lesser extent, by changing the rate of flow. The quenched sample is then collected and analyzed to quantitate the conversion of substrate to product (or intermediate), usually by chromatographic methods using radiolabeled substrates. The apparatus is then flushed and a new reaction loop is selected to obtain a different reaction time. By selecting various reaction loops, times from 2 to 100 msec can be obtained.

This simple design limits the maximum attainable reaction time by the maximum loop size. Longer reaction times cannot be obtained by using slower flow rates because it is necessary to use rapid rates of flow in order to maintain turbulence and efficient mixing. A 40-cm-long reaction loop, containing 200 μl of solution, provides a 100-msec reaction time. This design also wastes the often precious biological samples, by using enzyme and substrate to push the reactants through the reaction loop: at the end of each push, the reaction loop will contain 200 μl of reactants that must be discarded before the next run. In order to minimize sample volumes, to recover 200% of the reactants, and to achieve reaction

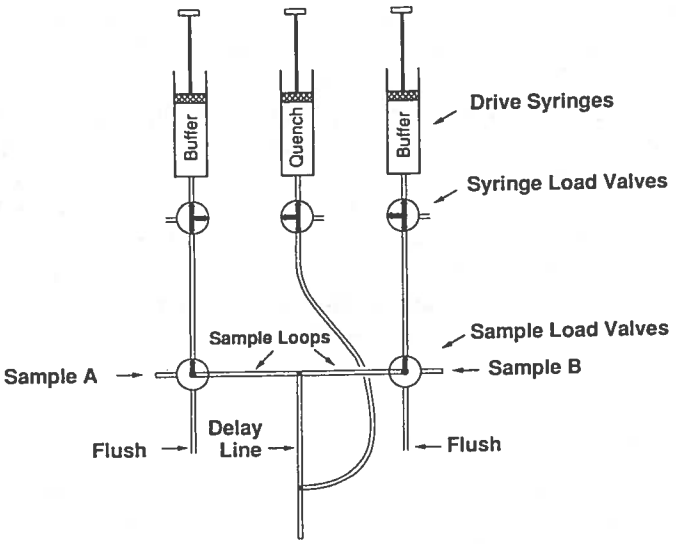

FIG. 3. Pulsed quench-flow apparatus.

times longer than 100 msec, we have redesigned the quench-flow according to the schematic shown in Fig. 3.

In this apparatus, enzyme and substrate are loaded into small loops of tubing containing 40 μl of solution. A three-way valve is then used to connect the loaded sample loop to a drive syringe containing buffer. The drive syringes are then used to force the reactants together and through the reaction loop to the point of mixing with the quenching solution and out into the collection tube. This apparatus allows collection of the entire sample and allows longer reaction times by operating in a push–pause–push mode. The first push is used to mix the reactants into the reaction loop, the pause allows the reaction to continue, and the second, timed push forces the reactants out of the reaction loop to be quenched and expelled into the collection tube. A three-way valve is used to allow loading and flushing of the contents of the reaction and sample loops between runs. By these methods, reaction times from 100 msec to 100 sec or longer can be obtained to complement the reaction times of 2–100 msec obtained in the direct push mode. A computer-controlled stepping motor provides the precise start–stop sequence. The use of an eight-way valve to select the appropriate reaction loop allows any reaction time to be selected conveniently. An entire reaction time course consisting of 25 time points can be collected from 1 ml of reactants in less than 1 hr. This apparatus made possible experiments to establish the reaction pathways of DNA polymerase (*10–12*), EPSP synthase (*3*, *31*), and tryptophan synthase (*32*).

IV. Kinetics of Substrate Binding and Catalysis

In this section, I will first describe experiments to measure each step in a simple reaction sequence (Scheme VI),

$$E + S \underset{k_{-1}}{\overset{k_1}{\rightleftharpoons}} E{\cdot}S \underset{k_{-2}}{\overset{k_2}{\rightleftharpoons}} E{\cdot}X$$

SCHEME VI

where E·X can represent an enzyme-bound product, intermediate, or a distinct conformation of the enzyme–substrate complex. I will then consider more complex reaction sequences, including the release of products from the enzyme. Multiple-substrate enzyme reaction sequences can be reduced to the simple scheme above by measuring the rate and equilibrium constants for the first substrates to bind and then considering the reaction of the second (or last) substrate according to Scheme VI.

A. ONE-STEP BINDING

If one has a signal for the binding of S to the enzyme and follows the progress of the reaction as it goes to completion, with substrate in excess over enzyme, the time dependence of the reaction can be fit to a single exponential. If we first consider an irreversible binding reaction

$$E + S \xrightarrow{k_1} E{\cdot}S \tag{6}$$

then the time dependence of the disappearance of E and appearance of E·S can be written:

$$\partial[E]/\partial t = -\partial[E{\cdot}S]/\partial t = -k_1[E][S] \tag{7}$$

If the concentration of substrate is in sufficient excess over enzyme, then [S] can be assumed to be a constant term giving a pseudo-first-order rate constant defined by the product, $k_1[S]$. Under these "pseudo-first-order" conditions the rate equation can be integrated to yield the time dependence of the reaction:

$$\begin{aligned} [E] &= [E_0]e^{-k_1[S]t} \\ [E{\cdot}S] &= [E_0](1 - e^{-k_1[S]t}) \end{aligned} \tag{8}$$

Thus, the free enzyme disappears and the enzyme–substrate complex appears with a time constant defined by the pseudo-first-order rate constant, $k_{obs} = k_1[S]$, obtained by fitting the reaction time course to a single exponential. The half-time for the reaction can be solved according to the time required to get $[E] = \frac{1}{2}[E_0]$, which gives $t_{1/2} = \ln 2/k_{obs}$.

When the concentrations of enzyme and substrate are comparable, the differ-

ential equations cannot be solved explicitly because both the enzyme and substrate concentrations vary with time. Under these and other conditions, computer simulation by numerical integration has been essential (see Section V,B).

We can now consider the fully reversible binding reaction. Under pseudo-first-order conditions with substrate in excess over enzyme, the rate equations can be integrated, yielding a form similar to Eq. (8):

$$[E]/[E]_0 = 1 - \frac{K_1[S]}{K_1[S] + 1}(1 - e^{-k_{obs}t})$$

$$[ES]/[E]_0 = \frac{K_1[S]}{K_1[S] + 1}(1 - e^{-k_{obs}t}) \qquad (9)$$

$$k_{obs} = k_1[S] + k_{-1}$$

where the amplitude term, $K_1[S]/(K_1[S] + 1) = [S]/(K_d + [S])$, is defined by the equilibrium concentration of ES. The first surprise is that the observed rate of reaction, as an exponential approach to equilibrium, is equal to the sum of the forward and reverse rates. This is a general rule that should be committed to memory because it applies to all reaction kinetics involving the approach to equilibrium. The basis for this phenomenon becomes apparent when one realizes that the amplitude of the reaction is reduced by the reverse reaction. When the reverse rate is negligible, the reaction goes to 100% completion and the observed rate is simply equal to $k_1[S]$. However, the back reaction reduces the amplitude of the reaction and thereby shortens the half-time for reaching equilibrium.

There are two important results from this analysis. First, the rate constants for binding and dissociation can be obtained from the slope and intercept, respectively, of a plot of the observed rate versus concentration. In practice this is possible when the rate of dissociation is comparable to $k_1[S]$ under conditions that allow measurement of the reaction. At the lower end, resolution of k_{-1} is limited by the concentration of substrate required to maintain pseudo-first-order kinetics with substrate in excess of enzyme and by the sensitivity of the method, which dictates the concentration of enzyme necessary to observe a signal. Under most circumstances, it may be difficult to resolve a dissociation rate less than 1 sec^{-1} by extrapolation of the measured rate to zero concentration. Of course, the actual error must be determined by proper regression analysis in fitting the data, and these estimates serve only to illustrate the magnitude of the problem. In the upper extreme, dissociation rates in excess of 200 sec^{-1} make it difficult to observe any reaction. At a substrate concentration required to observe half of the full amplitude, where $k_1[S] = k_{-1}$, the reaction would proceed toward equilibrium at a rate of 400 sec^{-1}. Thus, depending upon the dead time of the apparatus, much of the reaction may be over before it can be observed at the concentrations required to saturate the enzyme with substrate.

Within these limits, estimates of both the *on* and *off* rates can be obtained from a single experiment. However, in most instances other direct methods of estimating dissociation rates must be considered. Two methods are available and will be described below. First, substrate competition experiments can be performed by displacing the substrate with a tighter binding inhibitor or alternate substrate under conditions in which the rate-limiting step is the release of the bound substrate (Sections III,D,5 and III,D,6). Second, with multiple-substrate enzymes, the rate of dissociation of the first substrate can be estimated from substrate trapping experiments, measuring the kinetic partitioning between the forward reaction after binding of the second substrate and the reverse reaction by dissociation of the bound substrate (Section IV,F,2).

B. Two-Step Reaction Kinetics

The key to obtaining mechanistic information from transient kinetic methods is to examine the concentration dependence of the rates and amplitudes of the reaction. The concentration dependence reflects changes in the kinetics of binding and can reveal the presence of steps subsequent to binding that limit the rate of the observed reaction. The rate of binding is expected to increase linearly with increasing concentration of substrate with no signs of curvature. Curvature in the concentration dependence of the rate of a reaction is indicative of a two-step mechanism approaching a maximum rate that is limited by a first-order isomerization of the enzyme–substrate complex. For example, the binding of a substrate to an enzyme often occurs in two steps: the formation of a collision complex is followed by a change in state of the enzyme–substrate complex according to the following sequence:

$$E + S \underset{k_{-1}}{\overset{k_1}{\rightleftharpoons}} E{\cdot}S \underset{k_{-2}}{\overset{k_2}{\rightleftharpoons}} E{\cdot}X$$

where E·X may represent a distinct conformational state of the enzyme-bound substrate, an intermediate, or the enzyme-bound product of the chemical reaction. The observed kinetics of reaction will depend on the relative magnitudes of the four rate constants. We will first consider the rapid-equilibrium case and will then consider the complete solution to the two-step mechanism with all four rate constants.

1. *Rapid-Equilibrium Binding*

In many cases the rate of dissociation from the collision complex (E·S), defined by k_{-1}, is much faster than k_2, the rate-limiting chemical reaction or isomerization leading to tighter binding. Under these conditions the binding in step 1 comes to equilibrium on a time scale much faster than the first-order isomer-

ization. Accordingly, the first step can be simplified as a rapid-equilibrium reaction mechanism (Scheme VII).

$$E + S \overset{K_1}{\rightleftharpoons} E{\cdot}S \underset{k_{-2}}{\overset{k_2}{\rightleftharpoons}} E{\cdot}X$$

SCHEME VII

The solution of Scheme VII provides the time dependence of each of the three species:

$$\begin{aligned} [E]/[E]_0 &= \{1 - (K_1[S] + K_1K_2[S])/\alpha\}(1 - e^{-\lambda t}) \\ [ES]/[E]_0 &= (K_1[S]/\alpha)(1 - e^{-\lambda t}) \\ [EX]/[E]_0 &= (K_1K_2[S]/\alpha)(1 - e^{-\lambda t}) \end{aligned} \tag{10}$$

where the denominator of the amplitude term is defined by

$$\alpha = 1 + K_1[S] + K_1K_2[S]$$

The preexponential amplitude terms represent the concentration of enzyme in each form at equilibrium; for example, $[EX]/[E]_0 = K_1K_2[S]/(1 + K_1[S] + K_1K_2[S])$. The concentration dependence of the rate of reaction to form E·X follows a hyperbola, which is a function of the saturation of the initial collision complex:

$$\lambda = \frac{K_1k_2[S]}{K_1[S] + 1} + k_{-2} \tag{11}$$

The form of the equation exactly parallels that for Michaelis–Menten kinetics and for a similar reason. The increase in rate as a function of concentration reflects the saturation of the E·S collision complex; at the upper limit, the rate approaches the maximum rate of reaction. There are three important differences that distinguish these kinetic measurements from steady-state parameters: (1) the hyperbola is a function of the true dissociation constant, $K_d = 1/K_1$, because only a single turnover is measured; (2) the maximum rate provides a direct measure of the sum of the rate constants, $k_2 + k_{-2}$; and (3) the intercept on the y axis is equal to the rate constant, k_{-2}, defining the dissociation rate.

One should note that according to this mechanism the apparent second-order rate constant for substrate binding is given by the product K_1k_2 and the rate of dissociation of substrate will be limited by the rate constant k_{-2}. Thus the ratio of the *off* rate divided by the *on* rate is equal to the true dissociation constant even for this two-step reaction.

2. *Generalization: Kinetic Consequences of Rapid-Equilibrium Steps*

Whenever there is a step in a reaction sequence that can be considered to be in a rapid equilibrium, the two species in equilibrium become kinetically linked such that they are maintained in a constant proportion to each other. The rate of

reaction for species to leave the equilibrium is defined by the fraction of species in the reactive form times the intrinsic rate constant. The two (or more) enzyme species involved in the rapid equilibrium maintain a constant ratio as the reaction proceeds to completion.

3. *Examples: EPSP Synthase, Myosin, Tyrosyl-tRNA Synthetase, and DNA Polymerase*

The binding of shikimate 3-phosphate (S3P) and glyphosate (a potent, commercially important herbicide) to EPSP synthase provides a good example of two-step reaction kinetics with the first step in rapid equilibrium (*33*). S3P binds to the enzyme in a rapid equilibrium with rates of $k_{on} = 6.5 \times 10^8\ M^{-1}\ sec^{-1}$ and $k_{off} = 4500\ sec^{-1}$ (*3*). Glyphosate binds only to the enzyme–S3P complex and induces a change in protein fluorescence. Thus the kinetics follow a two-step reaction sequence (Scheme VIII),

$$E + S \overset{K_1}{\rightleftharpoons} E{\cdot}S \underset{k_{-2}}{\overset{k_2[G]}{\rightarrow}} E{\cdot}S{\cdot}G$$

SCHEME VIII

where the observable signal is a function of the formation of E·S·G. If S3P (S) and enzyme (E) are preincubated to allow saturation of E·S, and then mixed with glyphosate (G), the reaction follows a single exponential (Fig. 4A). As shown in Fig. 4B, the rate of the fluorescence change increases linearly with increasing concentration of glyphosate following the equation $k_{obs} = k_2[G] + k_{-2}$. The slope defines the second-order rate constant, $k_2 = 7.8 \times 10^5\ M^{-1}\ sec^{-1}$, and the intercept defines the dissociation rate of $k_{-2} = 0.12\ sec^{-1}$. Of course, the errors in estimating k_{-2} are quite large and the best estimate is based on a calculation of the *off* rate from the K_d and the *on* rate.

If the reaction is initiated by mixing various subsaturating concentrations of S3P with the enzyme and a fixed concentration of glyphosate, then the observed rate for the two-step reaction is defined by

$$k_{obs} = \frac{K_1k_2[S][G]}{K_1[S] + 1} + k_{-2} \tag{12}$$

A plot of rate as a function of S3P concentration follows a hyperbola (Fig. 4C) with an apparent $K_d = 1/K_1$, and a maximum rate defined by $k_2[G] + k_{-2}$. Thus, Eq. (12) reduces to the simple $k_{obs} = k_2[G] + k_{-2}$ at saturating concentrations of S3P.

In the example involving the binding of S3P and glyphosate, it was relatively easy to resolve the two-step reaction kinetics because of the separate concentration dependence for each step; the first step depended on S3P and the second on glyphosate. Moreover, substrate trapping studies established that S3P dissociates at a very fast rate (*3*), justifying the rapid equilibrium assumption. With the

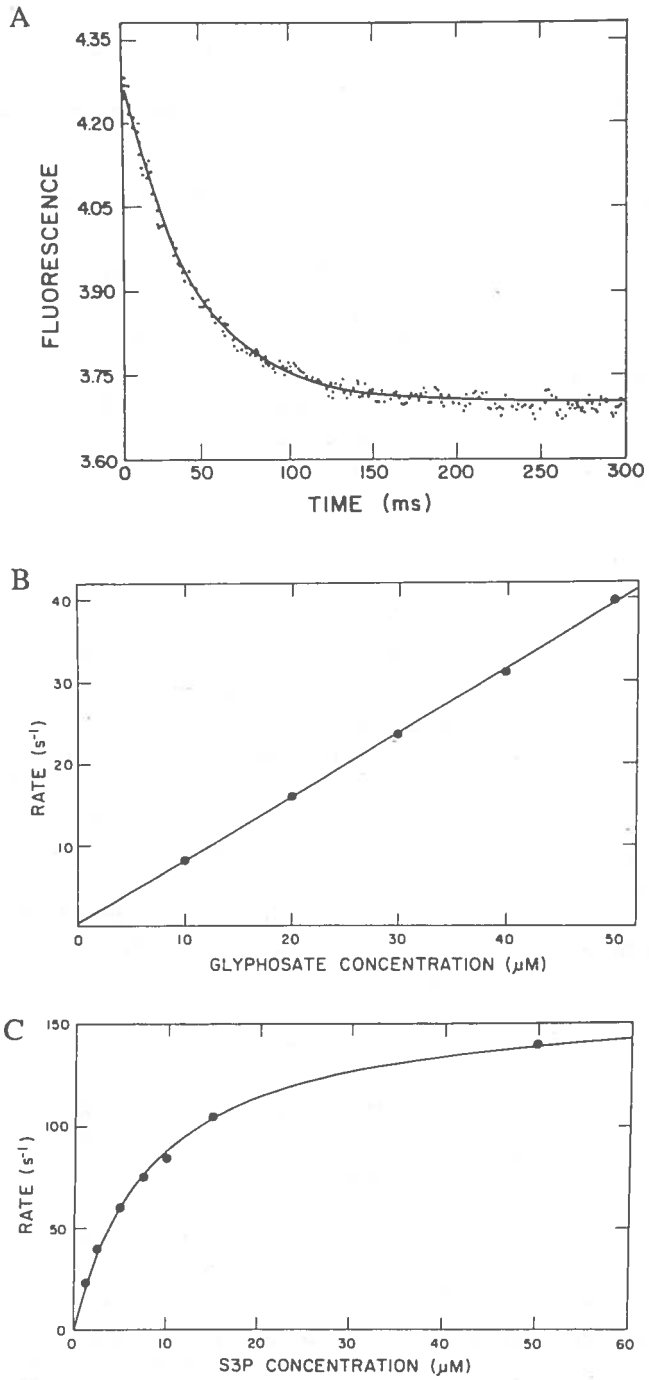

binding of a single substrate, it is reasonable to suggest that there is always some rearrangement of the E·S complex following the initial collision and leading to two-step binding kinetics. The important question becomes one of the rate of the rearrangement relative to the time resolution of the methods and the rate of catalytic turnover. On the one extreme, if the rearrangement following the initial collision simply involves the rotation of several bonds in the substrate, it may occur at rates in excess of 10^9 sec^{-1}, and would not be observed. In other cases, a conformational rearrangement after substrate binding may limit the rate of the chemical reaction. In practice, rapid mixing methods are limited to observation of rates slower than 1000 sec^{-1}, and so many fast rearrangements may go undetected and be of little physiological relevance.

A two-step binding mechanism is often invoked to explain an apparent second-order rate constant slower than diffusion. Estimates of the rate of diffusion-limited binding of a substrate to an enzyme active site vary considerably, but fall in the range of approximately 10^9 M^{-1} sec^{-1} (5). The apparent second-order rate constant for ATP binding to myosin has been measured to be 2×10^6 M^{-1} sec^{-1} and is attributed to an initial weak collision complex with $K_1 = 10^3$ M^{-1} followed by an isomerization at a rate of $k_2 = 2000$ sec^{-1}, providing an apparent second-order rate constant by the product $K_1 k_2$. Thus, if ATP binds at a rate of 10^8 M^{-1} sec^{-1}, it will dissociate from this weak collision complex at a rate of 10^5 sec^{-1}, effectively coming to equilibrium at a rate much faster than the first-order isomerization, leading to tighter binding.

In the myosin ATPase pathway, a second conformational change occurs at a rate of 100 sec^{-1}, which is followed by a faster chemical reaction (*30*). In the case of myosin, the conformational changes are responsible for the coupling of ATP binding energy to force production. For other enzymes, similar conformational rearrangements may be more common than is often recognized and may limit the observed rate of chemical reaction. For example, in extensive studies on tyrosyl-tRNA synthetase, the reaction of ATP with tyrosine to form the tyrosyl-AMP plus pyrophosphate was originally measured in single-turnover experiments and was described as the rate of the chemical reaction (*34*, *35*). Analysis of the crystal structure and quantitation of the kinetic effects of mutations in residues near the active site have provided evidence for a large change in struc-

FIG. 4. Kinetics of glyphosate binding to EPSP synthase. (A) The change in protein fluorescence at 340 nm was measured by stopped-flow methods after mixing enzyme (4.5 μM) with glyphosate (30 μM) and S3P (250 μM). The smooth line shows a fit to a single exponential with a rate of 4.5 sec^{-1}. (B) The glyphosate concentration dependence of the observed rate was measured in the presence of a saturating concentration of S3P (250 μM). (C) The S3P concentration dependence of the rate was measured in the presence of a fixed concentration of glyphosate (200 μM). Reproduced with permission from (*33*).

ture of a mobile loop that appears to limit the rate of the chemical reaction (*8*, *36*). Single-turnover kinetic analysis of DNA polymerase has also shown that the maximum rate of incorporation of dNTP is limited by a conformational change in the E·DNA·dNTP complex (*10–12*). This two-step binding mechanism largely accounts for the extraordinary specificity in recognition of the correctly base-paired dNTP during DNA replication.

C. Explicit Solution for Two-Step Reactions

We can first consider a simple two-step, irreversible mechanism:

$$E + S \xrightarrow{k_1} E{\cdot}S \xrightarrow{k_2} E{\cdot}X$$

For this simplified pathway, the time dependence of reaction is a double exponential. That is, for each species, E, E·S, and E·X, the time dependence follows an equation of the form

$$[E_i] = \alpha_1 e^{-\lambda_1 t} + \alpha_2 e^{-\lambda_2 t} + \gamma \tag{13}$$

where the observable rates are $\lambda_1 = k_1$ and $\lambda_2 = k_2$. This pathway is perhaps easy to relate to because each observable reaction rate corresponds to an intrinsic rate constant. However, it is rare that enzyme-catalyzed reactions are irreversible, and so this limiting case is not often useful.

For the more realistic, two-step reversible sequence

$$E + S \underset{k_{-1}}{\overset{k_1}{\rightleftharpoons}} E{\cdot}S \underset{k_{-2}}{\overset{k_2}{\rightleftharpoons}} E{\cdot}X$$

the solution to the time dependence of each enzyme species still follows a double exponential according to Eq. (15), but the amplitudes and the rates, λ_1 and λ_2, are dependent on all four rate constants. The full solution, including the amplitude terms for each species, is too complex to be useful except for the calculation of the predicted time course from a given set of kinetic constants, a task that can be done more easily by computer simulation as described below. The complete solution has been published elsewhere (*1*) and will not be repeated here. However, there are several important lessons to be learned from examination of the form of the equations for the rate of reaction, which can be applied in principle to any two-step reaction sequence.

The values of the rates λ_1 and λ_2 are defined by the roots of the quadratic equation:

$$\begin{aligned}\lambda_{1,2} = {} & (k_1 S + k_{-1} + k_2 + k_{-2}) \\ & \pm \{(k_1 S + k_{-1} + k_2 + k_{-2})^2 \\ & - 4[k_1 S(k_2 + k_{-2}) + k_{-1}k_2]\}^{1/2}\end{aligned} \tag{14}$$

Equation (14) can be simplified by the square root approximation (*1*) to yield

$$\begin{aligned}\lambda_1 &\simeq k_1[S] + k_{-1} + k_2 + k_{-2} \\ \lambda_2 &\simeq \frac{k_1[S](k_{-2} + k_2) + k_{-1}k_{-2}}{k_1[S] + k_{-1} + k_2 + k_{-2}}\end{aligned} \tag{15}$$

The fast phase of the reaction, λ_1, is equal to the sum of all four intrinsic first-order rate constants, defining the rate of formation of E·S and the decay of E. The substrate concentration dependence of the rate is a straight line with a slope equal to k_1 and an intercept equal to $k_{-1} + k_2 + k_{-2}$. The slow phase defines the rate of decay of E·S and the rate of formation of E·X, and the rate of slow decay of E if it is noticeably biphasic. The substrate concentration dependence of the slow reaction approximates a hyperbola with an apparent K_d defined by

$$K_d^{app} \simeq \frac{k_{-1}k_{-2}}{k_1(k_2 + k_{-2})} = \frac{K_d k_{-2}}{k_2 + k_{-2}} \tag{16}$$

and a maximum rate equal to $k_{max} = k_2 + k_{-2}$. The limiting slope at low substrate concentration defines the apparent second-order rate constant for binding,

$$k_{on} \simeq \frac{k_1[S](k_2 + k_{-2})}{k_{-1} + k_2 + k_{-2}} \tag{17}$$

and the intercept on the y axis is equal to the dissociation rate,

$$k_{off} \simeq \frac{k_{-1}k_{-2}}{k_{-1} + k_2 + k_{-2}} \tag{18}$$

Thus estimates of the apparent dissociation constant by calculation of the ratio of k_{off} divided by k_{on} will be equal to the K_d for step 1 if k_{-2} is large (relative to k_2 and k_{-1}), and will define the net dissociation constant for the two-step process, $K_d = 1/(K_1K_2)$, if k_{-2} is small relative to k_2. In any case, the estimated K_d will be within the limits

$$1/K_1 \geq K_d^{app} \geq 1/(K_1K_2) \tag{19}$$

and the calculated value will be an accurate estimate of the apparent K_d involving the actual distribution of species $E{\cdot}S \rightleftharpoons E{\cdot}X$ at equilibrium.

1. *Example: Tryptophan Synthase*

At first glance, Eq. (15) appears too complex to allow measurement of individual reaction rate constants. However, as we illustrate with this example, it is possible to extract estimates of all four rate constants from an analysis of the concentration dependence of the observed rates. The time dependence of reaction of serine with pyridoxal phosphate at the β-site of tryptophan synthase provides a good example of two-step reaction kinetics because of the unique optical

signals on reaction with pyridoxal phosphate (PLP). The serine first reacts with PLP to form an external aldimine (E·X), which then reacts further to form an aminoacrylate (E·A) (Scheme IX). The formation and decay of the aminoacrylate can be monitored by absorbance or fluorescence changes (*23–26, 32*). Figure 5A shows the time dependence of a change in fluorescence (exciting at 405 nm and observing emission at 500 nm). The data can be fit to a double exponential to extract the rates of each phase of the reaction (*32*). The concentration dependence of the fast and slow rates is shown in Fig. 5B. The fast phase follows a linear concentration dependence, extrapolating to a nonzero intercept in the limit of zero substrate concentration and showing no signs of reaching a maximum rate at high serine concentration. The slow phase approximates a hyperbolic function, reaching a maximum rate of 55 sec^{-1}.

These data fit two-step reaction kinetics according to Scheme IX.

$$E + S \underset{k_{-1}}{\overset{k_1}{\rightleftharpoons}} E{\cdot}X \underset{k_{-2}}{\overset{k_2}{\rightleftharpoons}} E{\cdot}A$$

SCHEME IX

The fast phase of the reaction occurs at a rate equal to the sum of all four rates in the pathway according to Eq. (15) (λ_1). The slope of the line defines $k_1 = 0.135\ \mu M^{-1}\ sec^{-1}$ and the intercept is equal to the sum $k_{-1} + k_2 + k_{-2} = 75\ sec^{-1}$. The slow phase of the reaction can be approximated by Eq. (15) (λ_2), which reaches a maximum rate equal to the sum $k_2 + k_{-2} = 55\ sec^{-1}$. Comparison of the intercept of the plot of the fast phase with the maximum rate of the slow phase yields an estimate of $k_{-1} = 20\ sec^{-1}$ from the difference. This analysis leads to definition of k_1, k_{-1}, and the sum $k_2 + k_{-2}$. Resolution of the contributions of the forward and reverse rates to the net rate, $k_2 + k_{-2}$, is based on an estimate of the absolute amplitude of the slow phase of the reaction and a fit to the concentration dependence of the slow reaction. Complete solution of the two-step reaction kinetics yielded all four rate constants: $k_1 = 0.135\ \mu M^{-1}\ sec^{-1}$, $k_{-1} = 20\ sec^{-1}$, $k_2 = 45\ sec^{-1}$, and $k_{-2} = 10\ sec^{-1}$.

In principle, the reaction of serine with the enzyme should have been written to include the formation of the collision complex between serine and the enzyme (E·S) (Scheme X).

$$E + S \underset{k_{-1}}{\overset{k_1}{\rightleftharpoons}} E{\cdot}S \underset{k_{-2}}{\overset{k_2}{\rightleftharpoons}} E{\cdot}X \underset{k_{-3}}{\overset{k_3}{\rightleftharpoons}} E{\cdot}A$$

SCHEME X

However, because the rate of the fast phase increased linearly without signs of curvature at high concentrations of serine, there is little information to define the binding of serine in the initial collision complex. The data suggest that the initial binding of serine is weak ($K_d > 20$ mM) and the rate of its reaction to form E·X is fast, compared to the attainable binding rates. For example, if the

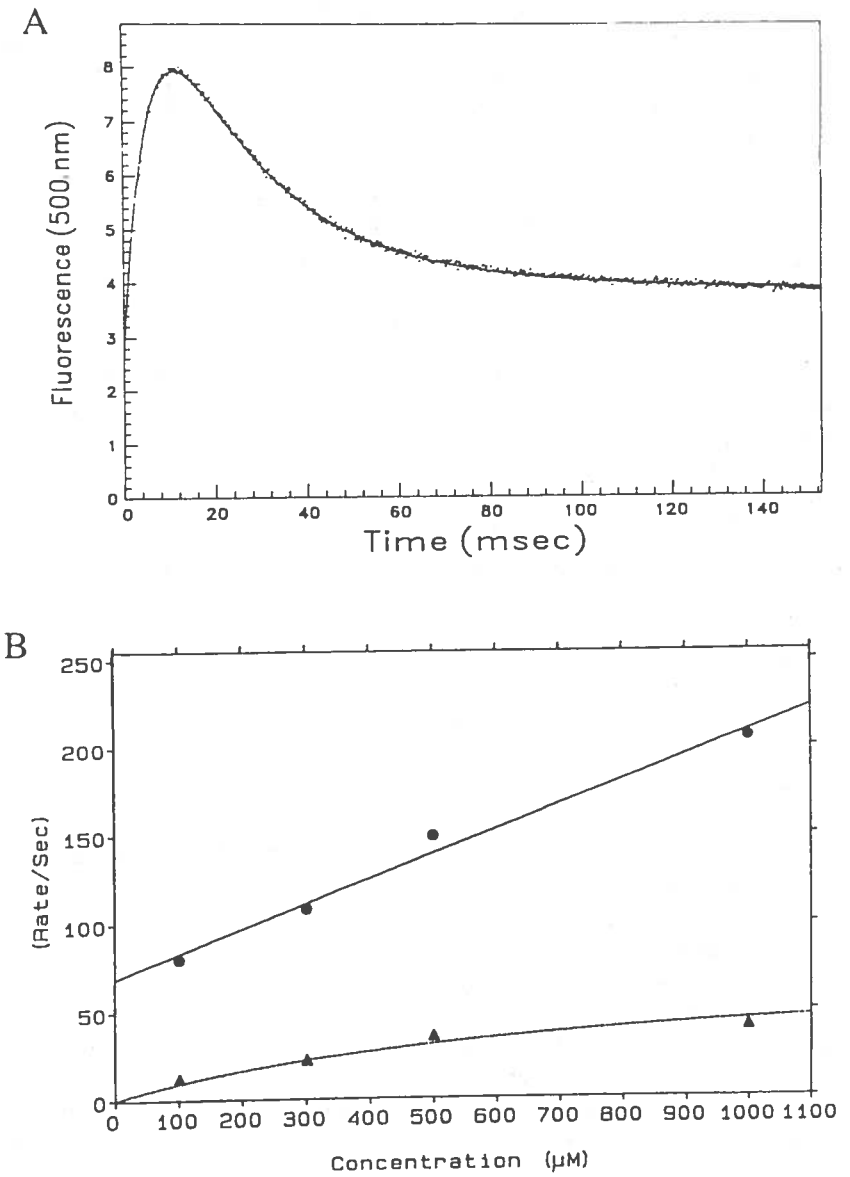

FIG. 5. Kinetics of serine reaction with tryptophan synthase. (A) The change in fluorescence at 500 nm was measured by stopped-flow after mixing enzyme (2 μM) with serine (500 μM). The smooth line represents a fit to a double exponential with rates of 150 and 40 sec^{-1}. (B) The serine concentration dependence of the fast and slow phases of the reaction are fit to the equations as described in the text. Reproduced with permission from (*32*).

K_d = 10 mM for the binding of serine, then k_2 = 1350 sec^{-1} is consistent with the observed rate of binding as the ratio k_2/K_d, and no curvature would have been apparent in the concentration dependence of the observed rate of the fast phase of the reaction at the highest concentrations of serine explored.

There have been significant advances toward the use of rapid-scanning stopped-flow, wherein the instrument can measure the absorption spectrum of the sample every 5 msec (*23*, *24*). This is of obvious value in helping to identify the species by their characteristic absorption spectra. However, it should also be apparent from the above analysis that the rates of reaction that are extracted by measurement at different wavelengths should be identical, provided that each reaction rate is represented. For example, in studies of the pyridoxal phosphate-catalyzed reaction of tryptophan synthase (*23*), measurements at 460 nm gave a single exponential at a rate of 136 sec^{-1}, while measurements at 430 nm gave a single exponential at a rate of 14 sec^{-1}. At 454 nm, a double exponential (rise–fall) was observed, which is a function of both rates. Thus the three experiments served to measure the same kinetically linked processes, with the different wavelengths providing a signal weighted toward one or both of the phases.

2. *Simulations of Two-Step Reactions*

In Fig. 6, we show simulations of the time dependence of E, E·S, and E·X according to the simple mechanism

$$E + S \underset{k_{-1}}{\overset{k_1}{\rightleftharpoons}} E{\cdot}S \underset{k_{-2}}{\overset{k_2}{\rightleftharpoons}} E{\cdot}X$$

with the rate constants defined in the figure legend. These simulations illustrate how the time dependence of the concentrations of each of the enzyme species is linked to other species in the pathway. Simulations were performed at four different concentrations of S. In Figs. 6B and 6C, the rise and fall of the intermediate species, E·S, can be clearly seen. At lower concentrations of S (Fig. 6A), the formation of E·S is rate limiting and so only a small amount of E·S ever accumulates (note longer time scale); E decays and E·X is formed according to a single exponential. At higher concentrations of S, the rate of formation of E·S is much greater than the reaction to form E·X (k_1[S] $\gg$ k_2, k_{-1}), and so E·S rises very rapidly and then decays in a single exponential as E·X is formed at a rate equal to $k_2 + k_{-2}$. Thus at both low and high concentrations of S, the intermediate species, E·S, is kinetically transparent if one measures the rate of formation of E·X which follows a single exponential.

At moderate concentrations of S, where the rate constants k_1[S] and the sum $k_2 + k_{-2}$ are *comparable*, one sees the rise and fall of the E·S species with the rate and amplitude of formation of E·S dependent on the magnitude of k_1[S] relative to k_2 (Figs. 6B and 6C). The formation of E·X proceeds with a lag phase

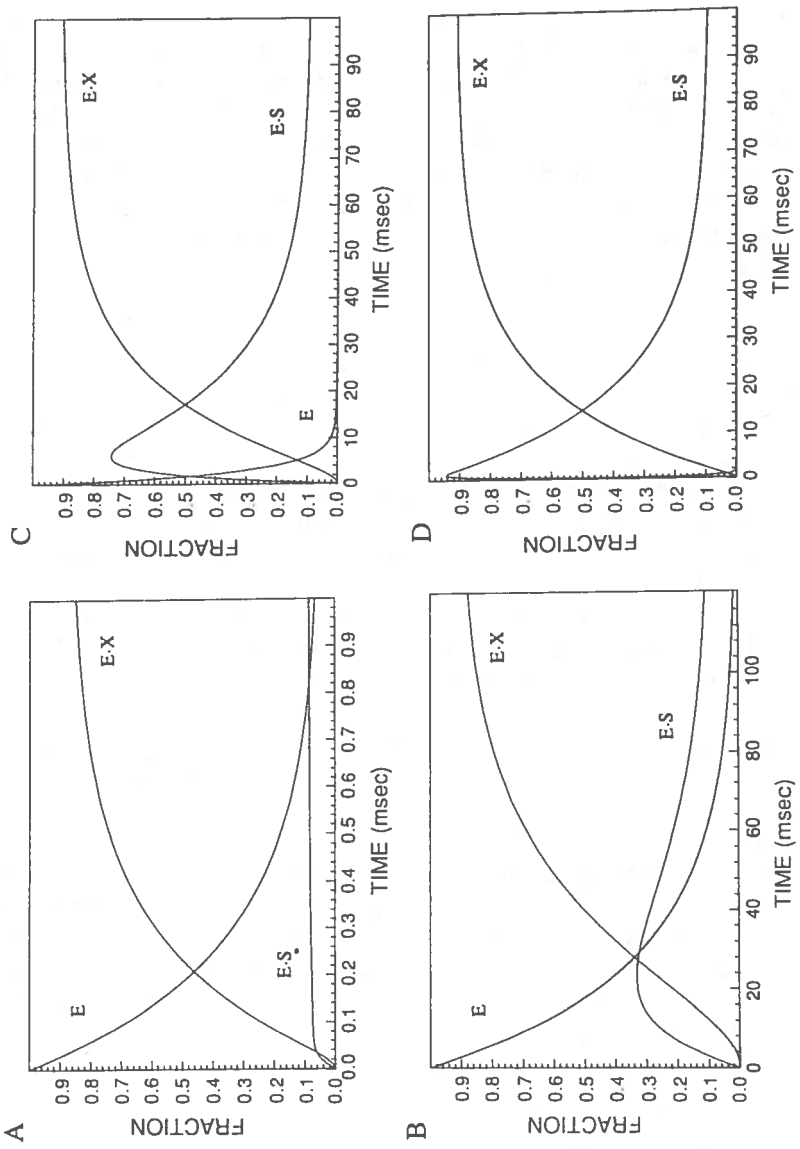

FIG. 6. Simulations of two-step reaction kinetics. Simulations of the two-step reaction kinetics according to Scheme VI were performed using the program KINSIM (*2*). The rate constants used were k_1 = 2 μM^{-1} sec^{-1}; k_{-1} = 2 sec^{-1}; k_2 = 50 sec^{-1}; k_{-2} = 5 sec^{-1}. Simulations were performed using 0.1 μM enzyme and various concentrations of substrate: (A) 2 μM; (B) 20 μM; (C) 200 μM; (D) 2000 μM.

that is a function of the rate of formation of E·S. The maximum rate of formation of E·X occurs when the peak in [E·S] is reached and the rate of reaching the peak in [E·S] is equal to the rate of approach to the maximum rate of formation of E·X. In mathematical terms, the time dependence of decay of E, formation of E·S, and formation of E·X each follow double exponentials [Eqs. (13) and (15)] and the rate constants governing each species are the same. The rate constant governing the rate of rise of E·S is the same as the rate constant defining the lag phase in the formation of E·X, and the rate of decay of E·S equals the rate of formation of E·X. Similarly, the fall of E is governed by the same two rate constants. At each concentration, the differences in the three curves for E, E·S, and E·X are only in the amplitude terms.

3. *Generalizations: Time Dependence of Two-Step Reactions*

There are two general conclusions from this analysis that can be applied to any multistep reaction sequence. First, the amplitude terms for each species, E, E·S, and E·X, are a function of all four rate constants. The rise and fall of the intermediate species, E·S, will be described by two exponential terms, one with a negative amplitude defining the rise and one with a positive amplitude defining the fall. At high substrate concentration (Fig. 6D), the amplitude governing the formation of E·S is large, but the rate of reaction is too fast to be observed, leading to collapse of the kinetics to resemble a one-step reaction. Under these conditions, the lag in formation of E·X is still there, but it is extremely short. Thus at low and high concentrations of S, the reaction to form E·X follows a single exponential; it is only at intermediate concentrations, where $k_1[S]$ is comparable to $k_2 + k_{-2}$, that a double exponential is observed with a lag phase in the formation of E·X. Stated in other terms, the observation of a lag in the kinetics implies that there are at least two steps in a reaction sequence that are comparable (within a factor of 10 in rate).

The second general conclusion from this analysis is that the time dependence for each of the species is governed by the same two rates, λ_1 and λ_2. Thus the fast phase of the fall of E and the rise of E·S and the lag prior to formation of E·X are all governed by one rate, λ_1. The fall of E·S and rise of E·X are governed by the other rate, λ_2. The time dependence of formation and decay of each species are kinetically linked to other species in the reaction sequence, such that they are all governed by the same set of rate constants. This is true for any mechanism.

4. *Resolving Rapid Equilibrium Steps*

It is often difficult to distinguish whether a two-step reaction can be fit assuming a rapid-equilibrium first step (Scheme VII) or whether it must be considered in terms of two steps of comparable rate (Scheme VI). The rapid-equilibrium

case is just one extreme, where $k_{-1} \gg k_2$, but in reality one must consider the case where the two rates are comparable. If the only observable signal is a function of the formation of E·X, then the rate of reaction, measured as a fit to a single exponential, will have a hyperbolic concentration dependence for either mechanism [Eq. (11) versus Eq. (15)]. In the rapid-equilibrium case, the fit to the hyperbola will provide an estimate of the K_d for the first binding step. However, if the reaction is not sufficiently rapid, the apparent K_d will be a function of all four rate constants [Eq. (15)]. There is one diagnostic feature of the reaction kinetics that distinguishes the two mechanisms. In the rapid-equilibrium case, the time dependence follows a single exponential at all substrate concentrations. In the general case, the time dependence of reaction will show a distinct lag when the rates of the initial binding and dissociation ($k_1[S]$ and k_{-1}) are comparable to the rate of relaxation of E·S to E·X ($k_2 + k_{-2}$). Careful examination of the reaction time course may reveal a lag in the reaction kinetics at low substrate concentrations. The lag is most prominent when the first reaction is 3- to 10-fold slower than the second reaction and will disappear when $k_1[S] > k_2 + k_{-2}$ as the substrate concentration increases. When two reactions in series occur at exactly the same rate, the kinetics are difficult to distinguish from a single exponential, and the observed rate of reaction is approximately half of the rate of either reaction.

5. *Kinetics of Ligand Exchange*

We can now consider the kinetics of ligand exchange with competition of two ligands for a single enzyme site according to the complete two-step reaction sequence (Scheme XI).

$$\text{E·A} \underset{k_{-1}}{\overset{k_1}{\rightleftharpoons}} \text{E} + \text{A}; \qquad \text{E} + \text{B} \underset{k_{-2}}{\overset{k_2}{\rightleftharpoons}} \text{E·B}$$

SCHEME XI

In general, the appearance of E·B will follow a double exponential with rates of

$$\lambda_1 \simeq k_1 + k_{-1}[\text{A}] + k_2[\text{B}] + k_{-2} \tag{20}$$

$$\lambda_2 \simeq \frac{k_1(k_{-2} + k_2[\text{B}]) + k_{-1}[\text{A}]k_{-2}}{k_1 + k_{-1}[\text{A}] + k_2[\text{B}] + k_{-2}}$$

As the concentration of B increases, the first relaxation, λ_1, will become too fast to measure and λ_2 will approach a maximum rate equal to k_1. In practice, extrapolation of the rate of exchange to an infinite concentration of B provides an estimate of the rate of dissociation of the E·A complex, k_1. This can often be accomplished by stopped-flow methods if the binding of A or B induces a distinct change in protein fluorescence.

6. *Example: Dihydrofolate Reductase*

The binding of substrates to dihydrofolate reductase follows the simple, one-step association reaction, which can be easily measured by the quenching of protein fluorescence that occurs on binding (*27*). Tetrahydrofolate (THF), for example, binds with a second-order rate constant of 25 μM^{-1} sec^{-1} and dissociates at a rate of 1.4 sec^{-1}. The slow rate of dissociation was accurately measured by mixing E·THF with methotrexate (MTX), a tight-binding inhibitor that quenches the protein fluorescence to a greater extent than THF, thus providing a signal in proceeding from E′·THF → E″·MTX. Under the appropriate conditions, the rate of the observable reaction is limited by the rate of dissociation of THF from the enzyme according to Scheme XII.

$$\text{E}'\cdot\text{THF} \underset{k_1}{\overset{k_{-1}}{\rightleftharpoons}} \text{E} + \text{THF}; \qquad \text{E} + \text{MTX} \underset{k_{-2}}{\overset{k_2}{\rightleftharpoons}} \text{E}''\cdot\text{MTX}$$

SCHEME XII

The experiment serves to measure k_{-1} because the binding of MTX, at the concentration used, is faster than the rebinding of THF ($k_2[\text{MTX}] \gg k_1[\text{THF}]$), and the binding of MTX is largely irreversible ($k_2[\text{MTX}] \gg k_{-2}$).

7. *Conformation Change Prior to Substrate Binding*

As an alternative to the substrate-induced conformational change that occurs after substrate binding, the mechanism according to Scheme XIII has been considered, with a conformational change preceding binding.

$$\text{E} + \text{S} \underset{k_{-1}}{\overset{k_1}{\rightleftharpoons}} \text{E}' + \text{S} \underset{k_{-2}}{\overset{k_2}{\rightleftharpoons}} \text{E}'\text{S}$$

SCHEME XIII

This mechanism can account for the saturation in the rate of binding with increasing substrate concentration, where the maximum rate is defined by k_1. It can also provide a rationale for an apparent second-order rate constant lower than the diffusion limit by a factor equal to the fraction of enzyme in the E′ state. How then can we distinguish this reaction pathway from the induced-fit model considered earlier (Scheme VI)?

First, if we consider that step 1 is a rapid equilibrium such that the E ⇌ E′ equilibrium is maintained throughout the progress of the reaction, then the rate of the forward reaction will be defined by the rate constant, k_2, times the fraction of enzyme in the E′ state. The reaction will approach equilibrium with a single exponential defined by $k^{obs} = K_1 k_2[\text{S}]/(K_1 + 1) + k_{-2}$. By this model, the apparent second-order rate constant for substrate binding is given by $K_1 k_2/(K_1 + 1)$. However, the rate will continue to increase with increasing substrate concentration and not reach a maximum according to this mechanism, with the rate constants k_1 and k_{-1} much larger than $k_2[\text{S}]$, the assumption for

a rapid-equilibrium mechanism. Thus, this model can account for any linear concentration dependence where the rate of binding is substantially below the diffusion limit. This mechanism may account for the remarkably low rate of phosphate binding seen for a number of enzymes, with values in the range of 10^4 M^{-1} sec^{-1} (*3*, *37*). The rebinding of phosphate, the product of the reaction, may indeed be constrained by the small fraction of enzyme in a proper conformation required for the enzyme–product state.

If the rate of the conformational change is slow enough to be observed, then one must consider the complete solution to the two-step reaction sequence, with the substrate concentration dependence in rate constant k_2 rather than k_1. Thus the time dependence of the reaction will follow a double exponential according to Eq. (13) but with the appropriate substitutions of the rate equations [Eq. (15)] to yield:

$$\lambda_1 \simeq k_1 + k_{-1} + k_2[\text{S}] + k_{-2} \qquad (21)$$

$$\lambda_2 \simeq \frac{k_1(k_{-2} + k_2[\text{S}]) + k_{-1}k_{-2}}{k_1 + k_{-1} + k_2[\text{S}] + k_{-2}}$$

To a first approximation, the fast phase will be due to the binding of S to E′, and the slow phase will then proceed by a rate that is limited by the rate constant k_1 at high substrate concentration. If the signal, such as a change in protein fluorescence, measures the sum of E′ + E′S, then the fast phase will not be observable and the data will follow a single exponential. If the signal measures the formation of E′S, then the reaction will show two distinct phases and the amplitude of the fast phase will be a function of the fraction of enzyme in the E′ state. The form of the equations is identical to that observed for the model invoking a conformational change subsequent to S binding. The two models cannot be distinguished on the basis of rate data alone, although the observation of different reaction rates with different substrates can be used to argue against this mechanism. In addition, the concentration dependence of the amplitude terms of the two phases could be used to distinguish the two models in some cases.

This example illustrates one of the limitations to the interpretation of stopped-flow kinetic data that must be kept in mind. The problem arises largely due to the fact that the extinction coefficients for kinetic intermediates may not always be known. Rigorous interpretation of kinetic data requires a knowledge of the absolute concentrations of species. For these reasons, chemical-quench-flow data can be more rigorously interpreted. On the whole, unless extinction coefficients of intermediates and products are known, stopped-flow experiments are much more difficult to interpret rigorously than quench-flow results. Stopped-flow experiments produce data of higher precision and can measure faster rates of reaction, but the quench-flow methods have distinct advantages by providing the absolute amplitudes of known chemical reactions.

D. Rules Governing Number of Exponential Terms

The integrated rate equations describing enzyme reaction pathways under first-order (or pseudo-first-order) conditions will always be a sum of exponential terms:

$$[E_i] = \sum \alpha_n e^{-\lambda_n t} + \gamma \tag{22}$$

Therefore, it is important to ask how many exponential terms can be expected for a given mechanism. The maximum number of exponentials defining the time dependence of a reaction can be estimated from the following rules:

1. There will be one exponential term for each step in a sequential reaction, with exceptions as defined below.
2. If substrate is in excess, product release from E·P to regenerate E does not lead to another exponential phase. Under these conditions, product release leads to the linear steady-state phase of the reaction and the rate of release contributes to the net rate of approach to steady state.
3. Any reaction that is much faster than the step preceding it will not be observable as a distinct step, but will occur at the rate of the preceding step. In mathematical terms, the fast step still leads to an exponential function in the integrated equation, but the term drops out of the expression at short times due to a fast rate.
4. Rapid-equilibrium steps do not contribute a kinetic step; the species in rapid equilibrium can be grouped together as a single, kinetic unit.

Thus according to these rules, the formation of E·P will follow a single exponential for the reaction sequence according to Scheme XIV, even though there are three steps.

$$E + S \overset{K_1}{\rightleftharpoons} E{\cdot}S \underset{k_{-2}}{\overset{k_2}{\rightleftharpoons}} E{\cdot}P \overset{k_3}{\rightarrow} E + P$$

Scheme XIV

At saturating [S] ([S] $\gg 1/K_1$), the maximum rate of approach of E·P to its steady-state concentration is $k_2 + k_{-2} + k_3$ for this model.

Scheme XV can be understood in terms of the simplified mechanism,

$$E + S \underset{k_{-2}}{\overset{k_1}{\rightleftharpoons}} E{\cdot}P \overset{k_3}{\rightarrow} E + P$$

Scheme XV

where the reaction of S to form E·P is approximated by the hyperbolic relationship:

$$\lambda_1 = \frac{K_1 k_2}{K_1[S] + k_2} \tag{23}$$

1. *Kinetics of Enzyme Inactivation*

The usefulness of knowing that the reactions of individual species are kinetically linked is illustrated by studies on the time dependence of enzyme inactivation in the presence of a slow-binding inhibitor or inactivator, for example. The reaction can be considered as

$$E_1 \overset{k_1}{\rightarrow} E_2$$

where E_1 and E_2 represent two enzyme forms catalyzing a reaction at two different rates:

$$S \overset{k_2[E_1]}{\rightarrow} P; \qquad S \overset{k_3[E_2]}{\rightarrow} P$$

By measuring the time dependence of product formation, the change in activity of the enzyme can be examined. The common method of data analysis is based on estimating the enzyme activity from the tangent to the curve at each time of reaction in a plot of product concentration versus time. However, this tedious and error-prone method of analysis can be avoided by recognizing that the time dependence of product formation will occur by an exponential followed by a linear phase:

$$[P] = A_0(1 - e^{-k_1 t}) + k_{ss} t \tag{24}$$

where k_{ss} represents the final steady-state rate. Thus, the rate of inactivation can be derived directly by analysis of the kinetics of product formation, without the intermediate step of attempting to estimate the rate of product formation at each time point along the progress of the inactivation. The rate of approach to the final linear phase, obtained as a fit to the exponential, will define the kinetics of inactivation directly, provided that the requirements of steady-state initial-velocity kinetics are maintained throughout the reaction time course. The amplitude of the exponential phase will depend on the rate of inactivation relative to the rate of catalysis by the fully active enzyme. Similar analysis can be applied to the case of a slow activation of an enzyme.

2. *Kinetics of Competing Reactions*

The kinetics of the partitioning of an enzyme-bound substrate to two products illustrates how the linkage between the two reactions leads to a single exponential. Consider the kinetics of a reaction pathway:

$$ES \overset{k_2}{\rightarrow} EP; \qquad ES \overset{k_3}{\rightarrow} EQ$$

According to this pathway, the rate of disappearance of ES and the rates of formation of EP and of EQ are each governed by a rate equal to the sum $k^{obs} = k_2 + k_3$. The kinetic partitioning between EP and EQ will only be re-

vealed by the relative amplitudes for formation of each product. For example, if $k_2 = 10\ \text{sec}^{-1}$ and $k_3 = 20\ \text{sec}^{-1}$, then the reactions will follow an exponential with $k^{obs} = 30\ \text{sec}^{-1}$, but one-third of the product will be P and two-thirds will be Q.

V. Measurement of Reaction Rates at Enzyme Active Sites

A. Presteady-State Burst Kinetics

When enzyme is first mixed with substrates (in excess over the enzyme), one can often observe a burst of product formation at a rate faster than steady-state turnover. This presteady-state burst is due to the accumulation of product at the active site of the enzyme. On quenching the reaction mixture with a denaturant to stop further reaction, the enzyme-bound product is liberated and the quantitation of product includes the sum of that bound to the enzyme and free in solution at the time of the quench.

Burst kinetics are often described in terms of a two-step irreversible mechanism (*5*, *38*).

$$E{\cdot}S \xrightarrow{k_2} E{\cdot}P \xrightarrow{k_3} E + P$$

The equation describing the time dependence of formation of product will be given by an exponential followed by a linear phase

$$\frac{[P]_{obs}}{[E_0]} = \frac{[EP] + [P]}{[E_0]} = A_0(1 - e^{-\lambda t}) + k_{cat}t \tag{25}$$

where the rates and amplitudes are defined by

$$\lambda = k_2 + k_3$$

$$A_0 = [k_2/(k_2 + k_3)]^2 \tag{26}$$

$$k_{cat} = k_2k_3/(k_2 + k_3)$$

The presteady-state burst will be followed by steady-state turnover at a rate given by k_{cat}. The presteady-state burst of product formation will occur at a rate defined by the sum of the rates of the chemical reaction and product release. The amplitude is also a function of both rate constants, k_2 and k_3. Thus, the amplitude of the burst can be predicted from the rate of the burst and the rate of steady-state turnover. Although this model can account for burst kinetics, it is often inadequate due to the assumed irreversibility of the chemical reaction. The internal equilibrium arising from the reverse of the chemical reaction (k_{-2}) reduces the amplitude of the burst to less than predicted by Eq. (26).

For a pathway including a reversible chemical reaction (Scheme XVI),

$$E{\cdot}S \underset{k_{-2}}{\overset{k_2}{\rightleftharpoons}} E{\cdot}P \xrightarrow{k_3} E + P$$

Scheme XVI

the time dependence of product formation still follows the general equation for burst kinetics

$$[P]_{obs}/[E_0] = A_0(1 - e^{-\lambda t}) + k_{cat}t \tag{27}$$

where the rates and amplitudes are defined by

$$\lambda = k_2 + k_{-2} + k_3$$

$$A_0 = k_2(k_2 + k_{-2})/(k_2 + k_{-2} + k_3)^2 \tag{28}$$

$$k_{cat} = k_2k_3/(k_2 + k_{-2} + k_3)$$

The rate of the burst is given by the sum of all three rate constants, and the amplitude is defined by the term, A_0. Thus, compared to the irreversible pathway, the rate of the burst will be faster and the amplitude will be lower, both due to the reversal of the chemical reaction. Estimates of all three rate constants can be obtained by proper fitting of the rate and amplitude of the presteady-state burst.

As the rate of product release increases, the amplitude of the burst decreases due to a lowering of the concentration of E·P present during steady-state turnover. It is important to remember that the rate of steady-state turnover is a simple function of $[E{\cdot}P]_{ss}$; namely, $k_{cat} = k_3[E{\cdot}P]_{ss}$. Thus, to a first approximation, the value of k_3 can be estimated from the slope of the time course divided by the intercept obtained by extrapolation of the linear phase to the y axis. This is not quite true because the intercept on the y axis, defining the amplitude of the burst, is less than the actual concentration of E·P present during the steady state: $[E{\cdot}P]_{ss} = k_2/(k_2 + k_{-2} + k_3)$. The burst amplitude is lower than the actual steady-state concentration of E·P by a factor equal to $(k_2 + k_{-2})/(k_2 + k_{-2} + k_3)$. Thus, a faster rate of product release, k_3, relative to the rate of the chemical reaction $k_2 + k_{-2}$, leads to a lower burst amplitude in the extrapolation.

The amplitude of the burst is governed by the rate of formation of E·P relative to the rate of release of P and the rate of back reaction to form E·S. The following rules can be applied to evaluate the amplitude of the burst:

1. The amplitude will be 1 per enzyme site provided that the formation of product is much faster than the rate of product release ($k_2 \gg k_3$) and the internal equilibrium favors E·P ($k_2 > k_{-2}$).
2. The amplitude will be reduced to be less than $[E{\cdot}P]_{ss}$ due to the competi-

tion between the rates of product formation and product release. As the rate of product release increases, the rate of approach toward steady state increases as the amplitude of the burst decreases. The amplitude will always fall between 0 and 1.

3. An amplitude less than that expected due to the observed rate of steady-state turnover and rate of the burst can be attributed to the internal equilibrium. Thus, as k_{-2} increases, the amplitude of the burst decreases and the rate of the burst increases.

4. If there is no burst, then either the chemical reaction or a step preceding the chemistry is rate limiting. Alternatively, the internal equilibrium may favor substrates ($K_1 \ll 1$); however, this is less likely due to the principles governing catalysis that tend to bring the equilibrium for a reaction closer to unity at the active site of the enzyme than in solution (*18*). In addition, a complete kinetic analysis would include examination of the burst in each direction, which could reveal an unfavorable equilibrium in one direction and a full burst amplitude in the opposite direction.

Because the amplitude of the burst is less than or equal to the concentration of enzyme sites, these experiments must be performed using enzyme concentrations that will produce measurable amounts of product in the first turnover. In order to saturate the rate of substrate binding so that chemistry, not binding, limits the rate of the burst, high concentrations of substrate must be used. The major experimental limitation of the method is due to the problems associated with measurement of less than one product per enzyme site with a background of excess substrate. Depending on the chromatographic resolution of the product from substrate, the ability to observe and measure a burst of product formation may be limited by accessible concentrations of enzyme.

Two assumptions underlie the derivations of the above equations. The first is that the rate of substrate binding is fast and is sufficiently favorable to saturate the enzyme sites on a time scale faster than catalysis. The second is that the release of products is presumed to be irreversible so that the concentration of product in solution can be neglected. In practice, neither of these assumptions limit the design or interpretation of experiments provided that the data are analyzed by numerical integration rather than by relying upon the explicit solutions provided here. By numerical integration, estimates of the rate constants governing the binding of substrate and product can be entered into the computer and included as part of the fitting process. The equations shown here should be used only to provide an initial fit to the data by nonlinear regression. These initial estimates of the constants can then be refined by more complete analysis based on computer simulation (*3*).

Even with computer simulation, it is still a concern that the rate of substrate binding must be faster than catalysis if the intent of the experiment is to measure

the rate of the chemical step. If substrate binding is much faster than catalysis ($k_1[S] \gg k_2$), the reaction proceeds toward steady state with a single exponential decay of E·S to E·P. However, if the concentration of substrate is lower, the rate of reaction to form E·P will be reduced according to the equations described for the two-step binding, and this will lead to a corresponding reduction in the amplitude of the burst. In the lower limit, the rate of the burst can provide a direct measurement of the rate of substrate binding, provided that product release is sufficiently slow. At moderate substrate concentrations, where $k_1[S]$ is only marginally faster than k_2 (less than 10-fold difference), there will be a lag in the production of E·P. In this case, it is still possible to extract reliable estimates of the rate of catalysis by including the rate of substrate binding in the data analysis by computer simulation (*2*, *3*, *39*).

B. Pulse-Chase Experiments

It is often possible to measure the kinetics of substrate binding by performing a kind of millisecond pulse-chase experiment in the quench-flow apparatus. The enzyme is first mixed with radiolabeled substrate, and then after a period of milliseconds is mixed with an excess of unlabeled substrate. After incubation for a brief period sufficient to convert all of the enzyme-bound substrate to products (six to eight turnovers), the reaction is stopped by the addition of acid, base, or other suitable quenching reagent. During the chase period, any tightly bound radiolabeled substrate is given sufficient time to be converted to product, while any loosely bound substrate or unbound substrate is diluted out by the excess of unlabeled material. According to this experimental protocol, one can measure the time dependence of formation of an enzyme–substrate complex. Of course, the method only permits detection of the fraction of enzyme–substrate complex that proceeds in the forward reaction, defined by the ratio $k_2/(k_2 + k_{-1})$ according to Scheme VI. The kinetics of reaction define the rate of formation of tightly bound substrate. Comparison of the reaction kinetics obtained in the pulse-chase experiment with that of a conventional acid-quench experiment can provide direct evidence for the formation of a tight enzyme–substrate complex preceding the chemistry step. For example, a pulse-chase experiment provided evidence for a tightly bound deoxynucleoside triphosphate involved in base pair recognition during DNA polymerization (*10*) and during ATP hydrolysis by myosin (*28*) or dynein (*37*, *39*), as described below (Section IV,B,1).

It is important to stress that I have used the term "tight" binding of the E·S complex in this context to refer only to the rate at which the substrate dissociates from the enzyme relative to the rate of reaction to form products. It is often the case that the binding of substrate in an initial, weak collision complex induces a change in enzyme conformation, resulting in a slower rate of substrate release and tighter binding (*29*, *40*). Nonetheless, it is important to keep in mind the

distinction between thermodynamic and kinetic stability. The experiment provides direct evidence for the kinetic partitioning of the E·S complex. It is only when this information is combined with measurements of the forward rate constants that estimates of thermodynamic stability can be obtained.

Examples: Mechanochemical ATPases

Studies on the dynein ATPase presented a particular challenge to the measurement of a presteady-state burst (*39*). During the course of studies on dynein, it was shown that molecular weight per ATPase site was approximately 750,000 and the maximum concentration of enzyme sites that could be obtained in solution was 1 μM. The steady-state turnover rate was 8 sec^{-1} and the second-order rate constant for binding ATP was 4×10^6 M^{-1} sec^{-1}. Thus a concentration of 30–50 μM ATP was required to obtain a sufficiently fast rate of ATP binding to observe a burst of product formation. Higher concentrations of ATP could not be employed because of the background due to the contaminating products of hydrolysis in every ATP preparation. A burst was observed, as shown in Fig. 7. In these experiments, the binding of ATP was still partially rate limiting and so the formation of product was biphasic with a slight lag phase. Data were fit using a minimal mechanism including all three steps—binding, chemistry, and product release (*39*).

Studies on kinesin established that the rate of ADP release limits steady-state turnover to an exceedingly slow rate in the absence of microtubules (0.009 sec^{-1}) (*41*). Therefore, as long as the rate of substrate binding (k_1[S]) is larger than the rate of ADP release, a burst can be observed. Hackney *et al.* took advantage of this fact to estimate the rate of ATP binding by measuring the rate of the burst at very low substrate concentrations, in the nanomolar range (*41*).

C. Single-Turnover Experiments

Because of the factors that reduce the amplitude in a presteady-state burst experiment and the difficulty in resolution of the product (or intermediates) from excess substrate, it is often desirable to use single-turnover methods. These experiments are performed with enzyme in excess over substrate to allow the direct observation of the conversion of substrates to intermediates and products in a single pass of the reactants through the enzymatic pathway. Unlike the presteady-state burst experiments, the kinetics are free of complications resulting from the steady-state formation of products, which limits the resolution of the burst kinetics and the detection of any intermediates above the background of excess substrates and products.

In a single-turnover experiment with enzyme in excess, the kinetics of the reaction are different than with substrate in excess. The rate of substrate binding

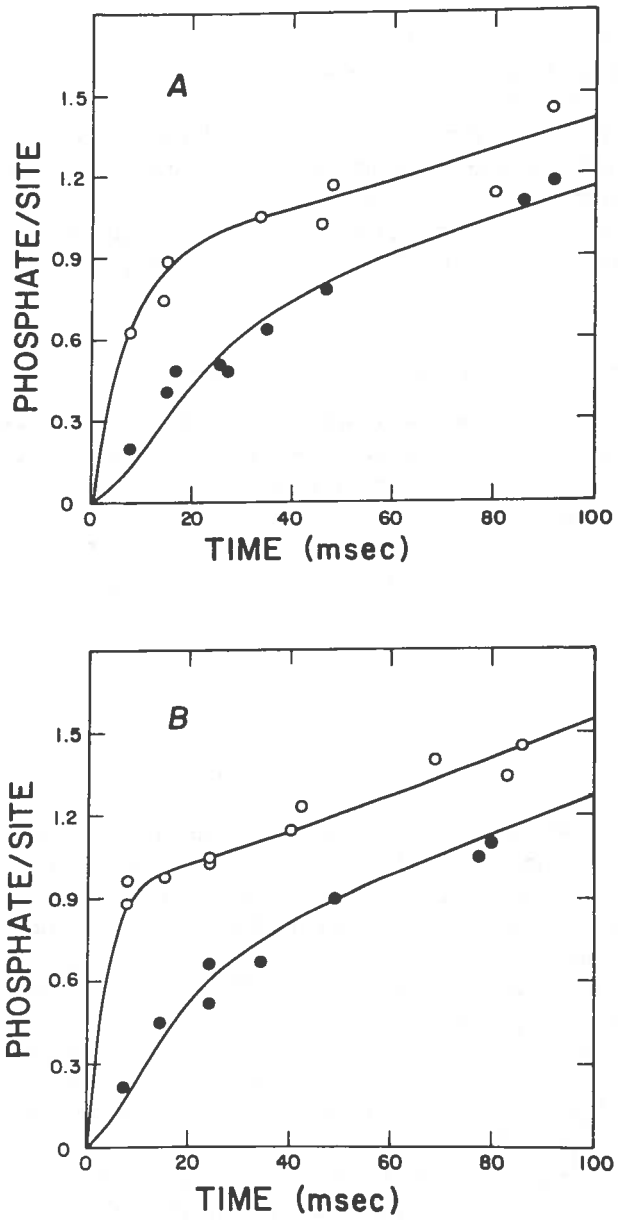

FIG. 7. Dynein ATPase burst kinetics. The kinetics of a presteady-state burst of ATP binding (○) and hydrolysis (●) were determined at two ATP concentrations: (A) 30 μM and (B) 50 μM. The data fit rate constants of $k_1 = 4.7$ μM^{-1} sec^{-1}, $k_2 = 55$ sec^{-1}, $k_{-2} = 10$ sec^{-1}, and $k_3 = 8$ sec^{-1} according to Scheme IV. Reproduced with permission from (*39*).

is governed by a pseudo-first-order rate constant defined by the product, $k_1[E]$. Thus if substrate binding is rate limiting, the rate of disappearance of substrate, obtained as an exponential fit to the time dependence of the reaction, will be independent of substrate concentration, but directly proportional to enzyme concentration. This is an important point that can be used to advantage in the design of experiments, although it also provides the major limitation of the method. The accessible concentrations of enzyme may limit the magnitude of $k_1[E]$ necessary to saturate the rate of substrate binding to measure the rate of the chemical reaction.

D. Observation of Enzyme Intermediates

The two-step reaction sequence discussed above can be translated directly to understand the reactions occurring at the enzyme site describing the formation and decay of an enzyme intermediate. For example, the enzyme sequence in Scheme XVII

$$E + S \underset{k_{-1}}{\overset{k_1}{\rightleftharpoons}} E{\cdot}S \underset{k_{-2}}{\overset{k_2}{\rightleftharpoons}} E{\cdot}I \underset{k_{-3}}{\overset{k_3}{\rightleftharpoons}} E{\cdot}P$$

Scheme XVII

will be reduced kinetically to Scheme XVIII

$$E{\cdot}S \underset{k_{-2}}{\overset{k_2}{\rightleftharpoons}} E{\cdot}I \underset{k_{-3}}{\overset{k_3}{\rightleftharpoons}} E{\cdot}P$$

Scheme XVIII

at concentrations of enzyme sufficient to saturate the rate and equilibrium for substrate binding in an experiment with enzyme in excess. Any enzyme concentration dependence observed for the rate of formation of the enzyme intermediate will reflect a rate-limiting substrate binding. At concentrations of enzyme sufficient to bind substrate at a rate faster than catalysis ($k_1[E] > k_2$), the kinetics of the reactions at the active site will then follow the questions described for a two-step reaction sequence [Eq. (15)].

Any fast reaction that follows a slow reaction will occur at the rate of the slow reaction. Consider the formation of an enzyme intermediate according to Scheme XVIII. This enzyme-bound intermediate (E·I) will be invisible kinetically and thermodynamically if $k_3 \gg k_2$ and $k_{-2} \gg k_{-3}$. Thus, one can only define the kinetically significant intermediates or conformational states. Transition states or extremely reactive intermediates cannot be directly observed; their presence can only be inferred by knowledge of the chemistry of the reaction. Alternatively, the use of alternate substrates or analogs has provided evidence for an intermediate by slowing the rate of the second step. For example, in studies on chymotrypsin, evidence in favor of an acyl intermediate was derived largely using reactive substrate analogs (*42*, *43*). In the normal physiological reaction, the formation of the acyl–enzyme intermediate is slow and is followed by a faster hydrolysis reaction. Therefore the acyl–enzyme cannot be observed. However, synthetic substrates were prepared that reacted rapidly to form the acyl–enzyme intermediate but were hydrolyzed more slowly, leading to the accumulation and identification of the intermediate.

Unique solution to the time dependence of formation and decay of the intermediate depends on an absolute measurement of its concentration. This is illustrated in Fig. 8, comparing the results of a simulation for a two-step irreversible mechanism,

$$E{\cdot}S \overset{k_2}{\rightarrow} E{\cdot}I \overset{k_2}{\rightarrow} E{\cdot}P$$

with the rate constants $k_2 = 100\ \text{sec}^{-1}$ and $k_3 = 20\ \text{sec}^{-1}$ (Fig. 8A) or with $k_2 = 20\ \text{sec}^{-1}$ and $k_3 = 100\ \text{sec}^{-1}$ (Fig. 8B). Note the lower amplitude for formation of the intermediate in the simulation in Fig. 8B. The same two simulations are shown superimposed in Fig. 8C, where a fivefold higher scaling factor (extinction coefficient) was used for the intermediate in the simulation involving the slower rate for k_2. This example illustrates clearly that the two pathways are indistinguishable unless the absolute concentration of the intermediate is known. The difficulty arises when the intermediate is unstable and its absolute concentration cannot be determined. However, even in this case, rapid-quench methods can measure the time dependence of formation and decay of the intermediate provided that it decomposes in the quench to yield products that can be uniquely identified (*3*, *44*).

Example: EPSP Synthase

The kinetics of formation and decay of a tetrahedral intermediate at the active site of EPSP synthase has been examined in both the forward and reverse directions, as shown in Fig. 9. The reaction catalyzed by EPSP synthase is an ordered, Bi Bi mechanism (Scheme XIX).

$$E + S3P + PEP \underset{k_{-1}}{\overset{k_1}{\rightleftharpoons}} E{\cdot}S3P + PEP \underset{k_{-2}}{\overset{k_2}{\rightleftharpoons}} E{\cdot}S3P{\cdot}PEP$$

$$E{\cdot}S3P{\cdot}PEP \underset{k_{-3}}{\overset{k_3}{\rightleftharpoons}} E{\cdot}I \underset{k_{-4}}{\overset{k_4}{\rightleftharpoons}} E{\cdot}EPSP{\cdot}P_i$$

$$E{\cdot}EPSP{\cdot}P_i \underset{k_{-5}}{\overset{k_5}{\rightleftharpoons}} E{\cdot}EPSP + P_i \underset{k_{-6}}{\overset{k_6}{\rightleftharpoons}} E + EPSP + P_i$$

Scheme XIX

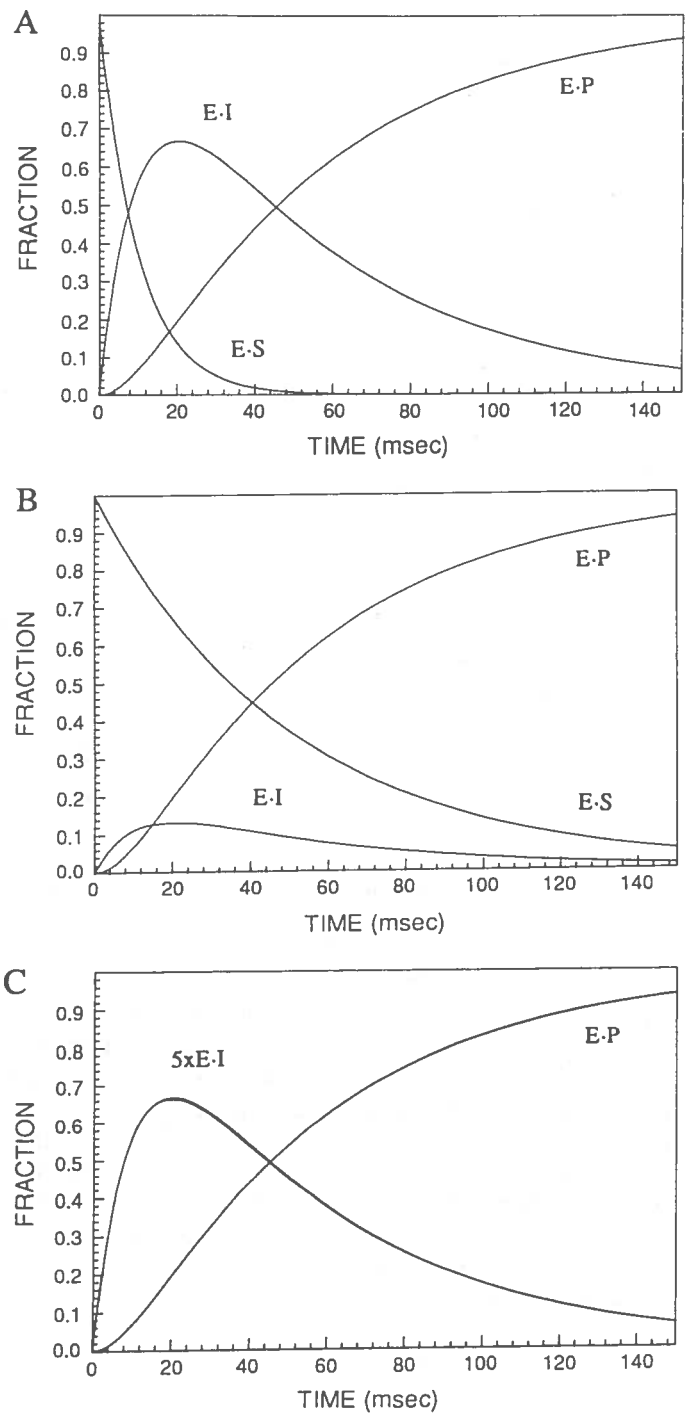

Figure 9A shows the reaction in the forward direction in a single-turnover experiment tracing the conversion of radiolabeled phosphoenol pyruvate (PEP) to intermediate (I) and then EPSP with enzyme in excess over the limiting substrate. The enzyme was first saturated with S3P and the reaction was initiated by the addition of labeled PEP. The intermediate was formed within 3 msec and decayed to EPSP over the next 30–40 msec. Figure 9B shows the reverse reaction, which was initiated by mixing radiolabeled EPSP with enzyme and an excess of phosphate. The kinetics show the transient appearance of the intermediate in equilibrium with EPSP at the active site; the intermediate and EPSP decay in constant proportion as the products, PEP and S3P, are formed. The fit to the data led to a unique set of rate constants accounting for the time dependence of appearance and disappearance of the intermediate in both the forward and reverse reactions, with $k_3 = 1200\ \text{sec}^{-1}$, $k_{-3} = 100\ \text{sec}^{-1}$, $k_4 = 320\ \text{sec}^{-1}$, and $k_{-4} = 240\ \text{sec}^{-1}$ Initial fitting of the rapid-quench data was based on use of an acid quench, which caused the intermediate to break down to yield pyruvate. Subsequent work, using a quench with neat triethylamine, allowed isolation and identification of the intermediate and measurement of the internal equilibrium constants (K_3, K_4) for its formation at the active site (*3, 16*).

The reactions in each direction illustrate the need for computer simulation to interpret quantitatively the reaction kinetics. In the forward direction, the binding of PEP was largely rate limiting and constrained by other experiments to be no greater than $k_2 = 15\ \mu M^{-1}\ \text{sec}^{-1}$. Thus, in the fitting of the data, the rate of reaction to form the intermediate was limited to a rate of $300\ \text{sec}^{-1}$ for PEP binding (k_2[E]) followed by $1200\ \text{sec}^{-1}$ for the chemical reaction. Combined with the measurement of the internal equilibrium constant (K_3) and the rate of the single turnover in the reverse direction, confidence in the estimate of $k_3 = 1200\ \text{sec}^{-1}$ is beyond what could have been achieved by a single experiment. It is the combination of all experiments together that allows the unique fit to the reaction kinetics and defines the pathway.

In the reverse reaction, driving the synthesis of S3P and PEP from EPSP and phosphate, the amplitude of the product formation was altered because of the formation of a dead-end complex with S3P and phosphate bound to the active site. The time dependence of this inhibition during the single turnover to form E·S3P would lead to a model too complex to solve explicitly. The reaction time

FIG. 8. Importance of amplitude information. The kinetics of a two-step irreversible reaction sequence were simulated using KINSIM (2). (A) $k_1 = 100\ \mu M^{-1}\ \text{sec}^{-1}$; $k_2 = 20\ \text{sec}^{-1}$. (B) $k_1 = 20\ \mu M^{-1}\ \text{sec}^{-1}$; $k_2 = 100\ \text{sec}^{-1}$. (C) The results of the two simulations from **A** and **B** are superimposed with a scaling factor of 5× multiplied by the concentration of E·I for the second simulation (**B**). These simulations show that the two kinetic pathways in **A** and **B** are indistinguishable in the absence of absolute amplitude information.

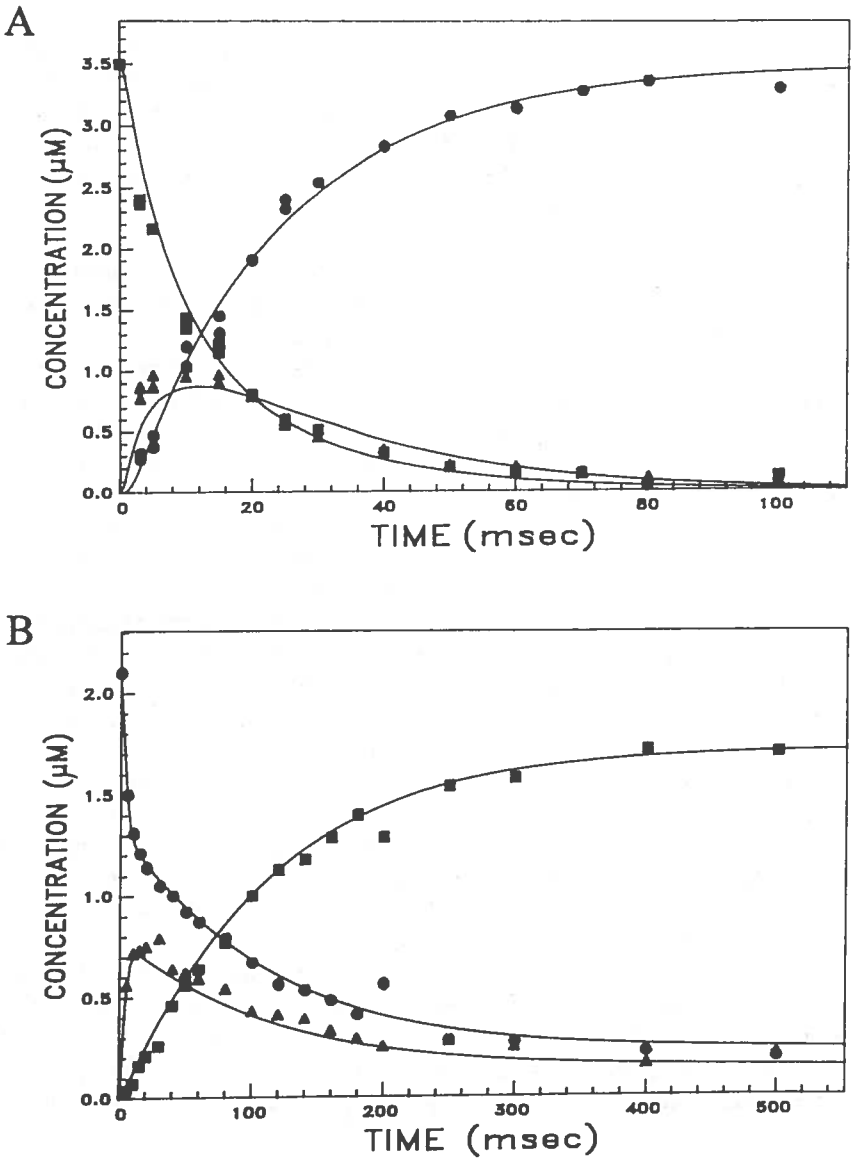

FIG. 9. EPSP synthase single-turnover kinetics and EPSP synthase reaction pathway. (A) The disappearance and formation of PEP (●), EPSP (■), and intermediate (▲) were monitored in the reverse direction. The reaction was initiated by mixing enzyme (10 μM) and S3P (100 μM) with radiolabeled PEP (3.5 μM). (B) The disappearance and formation of EPSP (●), PEP (■), and intermediate (▲) were monitored in the reverse direction. The reaction was initiated by mixing enzyme (10 μM) with phosphate (7.5 μM) and radiolabeled EPSP (2.1 μM). The curves were calculated by computer simulation using the fill kinetic pathway shown in Scheme XIX and the 12 individual rate constants (*3*). Reproduced with permission from (*3*).

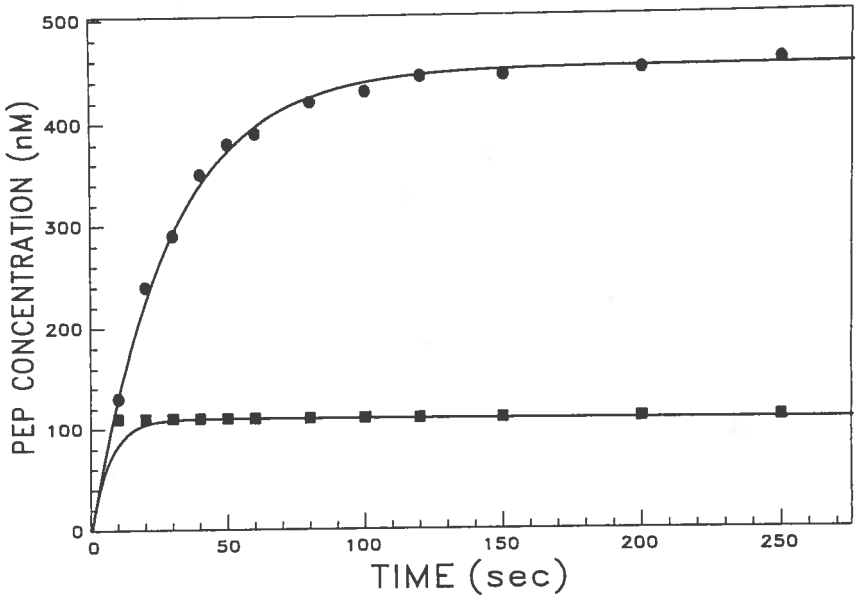

FIG. 10. Kinetics of phosphate binding to EPSP synthase. The reaction was run in the absence (●) and presence (■) of unlabeled PEP. The reaction was initiated by mixing enzyme (5 μM) with radiolabeled phosphate (0.5 μM) and excess EPSP (1 mM). The curves were calculated by computer simulation using the full kinetic pathway shown in Scheme XIX and the 12 individual rate constants (*3*). Reproduced with permission from (*3*).

course is easy to analyze by including in the computer simulation the reaction steps leading to formation of the nonproductive complex.

The rate of phosphate binding to EPSP synthase was measured by a single-turnover experiment in the reverse reaction shown in Fig. 10. The experiment was initiated by mixing an excess of enzyme and EPSP with a trace of labeled phosphate (<1 μM). Under these conditions, the rate of formation of PEP was limited by the rate of phosphate binding to the enzyme–EPSP complex. However, in the absence of unlabeled PEP, the reaction did not go to completion. Successful execution of this experiment required the addition of the unlabeled reaction product (PEP) in order to ensure that the release of radiolabeled PEP was irreversible. In the absence of unlabeled PEP, the reaction came to equilibrium short of complete conversion of radiolabeled phosphate to PEP. The addition of unlabeled PEP "pulled" the reaction to completion by dilution of the radiolabeled PEP. Computer simulation was required to analyze quantitatively the reaction time course. Conventional data fitting to the time dependence of the reaction gives a rate of approximately 0.035 sec^{-1}. The simple interpretation would then lead to calculation of a second-order rate constant for phosphate

binding of 0.007 μM^{-1} sec^{-1}. However, computer simulation leads to an estimate of 0.07 μM^{-1} sec^{-1}. The difference is due to the fact that the computer simulation accounts for all of the steps of the reaction. Although this experiment provides information that is largely a function of the rate of phosphate binding, the reverse reaction and the other steps in the pathway, which are measured more accurately by other experiments, have a secondary effect on the time dependence of the reaction. Inclusion of the complete reaction sequence in the fitting of these data provides the most accurate estimate of the binding rate that is consistent with all of the experimental evidence.

E. Kinetics of Substrate Channeling

The channeling of metabolic intermediates between pairs of sequential enzymes in a reaction pathway is a controversial topic (*45–47*). Kinetic evidence for the direct passage of a metabolite from one enzyme to the next has been based largely on indirect tests in the steady state (*48–50*). Recently the problem has been addressed by direct measurement of the rate of exchange (*51–53*). A proper comparison with rates of substrate binding and dissociation establishes whether the rates of exchange are consistent with the dissociation–rebinding pathway, or whether one is forced to suggest a direct transfer between the two enzyme active sites.

The kinetics of exchange of a single ligand between two enzymes can be considered according to the pathway shown in Scheme XX.

$$E_1{\cdot}A \underset{k_{-1}}{\overset{k_1}{\rightleftharpoons}} E_1 + A; \qquad E_2 + A \underset{k_{-2}}{\overset{k_2}{\rightleftharpoons}} E_2{\cdot}A$$

Scheme XX

The complete solution will again follow a double exponential, which can be reduced to a single exponential depending on the rates of reaction.

$$\lambda_1 \simeq k_1 + k_{-1}[E_1] + k_2[E_2] + k_{-2} \tag{29}$$

$$\lambda_2 \simeq \frac{k_1(k_{-2} + k_2[E_2]) + k_{-1}[E_1]k_{-2}}{k_1 + k_{-1}[E_1] + k_2[E_2] + k_{-2}}$$

Because it is unlikely that the rates of reaction will differ greatly in comparing the two enzymes and because there are practical limits to the concentration of enzyme E_2 that can be used, the complete solution to the two-step reaction must be considered in analyzing data.

Application of these methods to the channeling of NADH between glycerol phosphate dehydrogenase (GDH) and lactate dehydrogenase (LDH) has produced conflicting results (*51, 54*). The initial results showed that the rate of exchange was faster than the rate of dissociation of NADH from GDH, and therefore it was concluded that NADH must have been transferred directly from the active site of GDH to LDH (*54*). However, it is important to note that the rate of ligand exchange, according to the equations described above, will be greater than the dissociation rate. At the concentrations of LDH accessible in solution, the displacement NADH from GDH is incomplete and the reaction reaches an equilibrium. The observed rate of approach to equilibrium is a function of the sum of the forward and reverse rates. By overlooking this fundamental property of transient kinetics, the authors were led to the wrong conclusion (*54*). A more rigorous analysis has shown that the rates of transfer are entirely consistent with a free diffusion model, involving dissociation of NADH from GDH and rebinding to LDH, rather than requiring a direct transfer (*51*).

Example: Tryptophan Synthase

The kinetics of metabolite channeling have been examined most thoroughly by application of single-turnover kinetic methods in the case of tryptophan synthase. Tryptophan synthase catalyzes the last two reactions in the pathway for tryptophan biosynthesis as shown in Fig. 11 (*55*). Indole, the product of the cleavage of indoleglycerol phosphate (IGP) at the α-site, is thought to pass through a channel in the enzyme to react with serine at the β-site in a pyridoxal phosphate-dependent reaction. Solution of the crystal structure revealed the presence of a 25-Å-long tunnel through the enzyme connecting the α- and β-sites (*55*). Evidence for the passage of indole through the tunnel was obtained by stopped-flow studies with analogs (*56, 57*) and analysis of the kinetics of tryptophan formation from indoleglycerol phosphate in a single turnover with enzyme in excess over the radiolabeled IGP (*32*). As shown in Fig. 12, the formation of tryptophan occurs without significant appearance of indole from IGP. This result implies that indole must diffuse to the β-site and react quite rapidly, with an overall rate of least 1000 sec^{-1}. Measurement of the rate of reaction of indole added from solution established a rate of only 40 sec^{-1} under conditions identical to the reaction with IGP. Computer simulation established that if the indole had to dissociate from the α-site, diffuse through solution, and rebind to the β-site, then a large fraction of indole should have accumulated in the single-turnover experiment, as shown by the dashed line in Fig. 12. Thus, the kinetic measurements establish that the indole must have passed through the tunnel to account for the exceedingly fast reaction rate and the negligible accumulation of indole (*32*).

Further analysis of the reaction kinetics showed that there is a communication from the β-site to the α-site (*32*). In the absence of serine, the α-site is relatively inactive in catalyzing the cleavage of IGP (0.16 sec^{-1}). The reaction of serine with pyridoxal phosphate at the β-site to form the highly reactive aminoacrylate

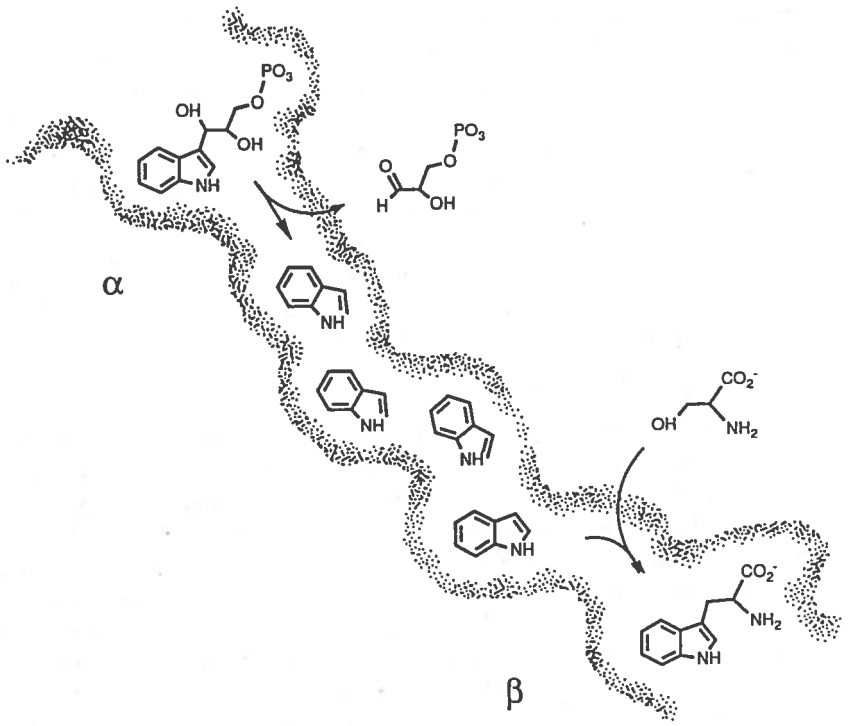

FIG. 11. Channeling in the tryptophan synthase reaction. Indoleglycerol 3-phosphate is cleaved to indole and glyceraldehyde 3-phosphate at the α-site. Indole is then passed through the hydrophobic channel to the β-subunit where it reacts with serine to form tryptophan. This schematic was drawn from data presented in (*55*).

leads to a 200-fold activation of the rate of IGP cleavage at a distance 25 Å away at the α-site. When serine and IGP are added simultaneously to the enzyme, there is a lag in the kinetics of IGP cleavage and tryptophan formation, which parallels the kinetics of formation of the aminoacrylate. When serine is preincubated with the enzyme, the lag is no longer seen when the reaction is initiated by adding IGP. Thus, direct analysis of the reaction kinetics revealed novel features of substrate channeling. The channeling of indole from the α-site to the β-site is efficient for two reasons. First, the intersubunit communication precludes the formation of indole in the absence of serine and serves to keep the reactions at distant sites in phase. Second, the passage of the indole through the tunnel and its reaction with the aminoacrylate to form tryptophan are much faster than the rate of release of indole from the α-site. The application of single-

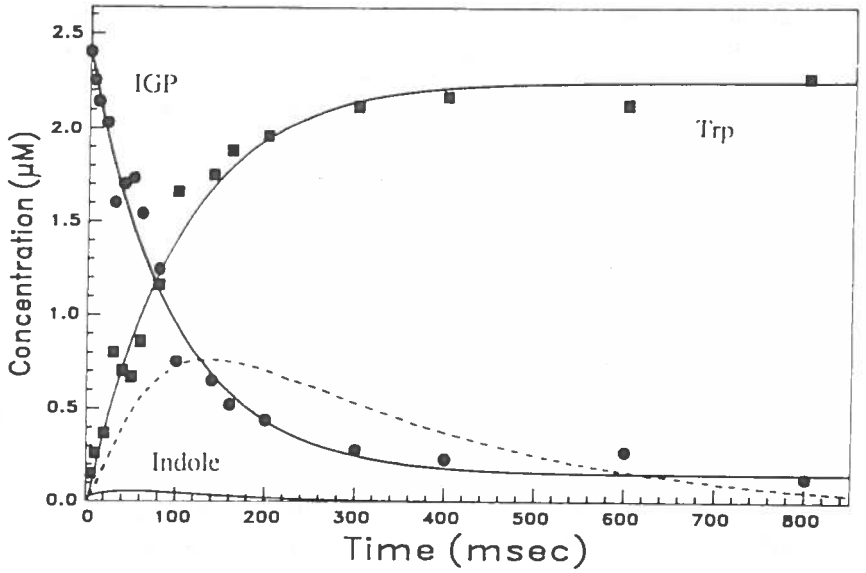

FIG. 12. Tryptophan synthase single turnover. A solution of serine and enzyme was mixed with indoleglyerol phosphate (IGP) to initiate the reaction. The disappearance and formation of IGP (●) and tryptophan (Trp; ■) were monitored. The reaction was initiated by mixing enzyme (20 μM) and serine (10 mM) and radiolabeled IGP (2.4 μM). The curves were calculated by computer simulation using the full kinetic pathway (*32*). For the dashed line, the curves were simulated using a rate of indole binding equal to 20 μM^{-1} sec^{-1} (40 sec^{-1} at 20 μM enzyme), predicting a substantial accumulation of indole. Reproduced with permission from (*32*).

turnover kinetic methods to other enzyme systems thought to exhibit channeling should reveal whether these properties are of general importance in governing channeling of metabolic intermediates.

F. KINETIC PARTITIONING

The kinetic partitioning of enzyme intermediates is an important principle, and the rules governing kinetic partitioning are quite simple. The fractional yield of a given reaction is given simply as the rate of the desired reaction divided by the sum of the rates of all reactions involving the intermediate. For example, consider the forked reaction pathway in Scheme XXI.

$$E{\cdot}S \underset{k_{-1}}{\overset{k_1}{\rightleftharpoons}} E{\cdot}I \begin{matrix} \overset{k_2}{\nearrow} E + P \\ \underset{k_3}{\searrow} E + Q \end{matrix}$$

SCHEME XXI

According to this mechanism, the fractional yield of the intermediate to form P is given by the ratio $k_2/(k_2 + k_{-1} + k_3)$. The importance of kinetic partitioning will be illustrated by two examples.

1. *Substrate Trapping Experiments*

For a sequential bisubstrate enzyme, the rate of dissociation of the first substrate can be estimated by substrate trapping methods. The rationale for this experimental approach is shown in Scheme XXII. The enzyme is first preincubated with radiolabeled substrate A* and is then mixed with an excess of unlabeled substrate A and substrate B to initiate the reaction. The recovery of radiolabeled product is a function of the kinetic partitioning of the enzyme-bound substrate between dissociation to yield free S and forward reaction with substrate B to yield product P.

$$\begin{array}{l} \mathrm{E{\cdot}A^*} \overset{k_2[\mathrm{B}]}{\underset{k_{-2}}{\rightleftharpoons}} \mathrm{E{\cdot}A^*{\cdot}B} \rightarrow \mathrm{E{\cdot}Q^*{\cdot}P} \rightarrow \mathrm{E} + \mathrm{Q^*} + \mathrm{P} \\ \quad k_{-1} \downarrow \\ \quad \mathrm{E} + \mathrm{A^*} \end{array}$$

SCHEME XXII

Quantitative analysis of the reaction is based on examining the effect of increasing concentrations of B on the recovery of radiolabeled product. In the limit, extrapolating to infinite concentration of B, one expects 100% conversion of the enzyme-bound radiolabeled substrate to product. Recoveries less than 100% have been attributed to dissociation of A* from the ternary E·A*·B complex, nonproductive binding of A* in the E·A* complex, or an appreciable fraction of dead enzyme. In addition, the analysis is dependent on an accurate knowledge of the equilibrium constant for the binding of the substrate A to the enzyme and of the concentration of *active* enzyme sites. Independent of these concerns, one can estimate the rate of dissociation of A from the enzyme by measurement of the concentration of B required to trap half of the maximal amount of radiolabeled A*. At this concentration, the rate dissociation of A* from the E·A* complex is equal to the rate of binding of B. Such analysis was used to estimate the rates of dissociation of S3P and EPSP from the enzyme EPSP synthase (*3*).

2. *DNA Polymerase Error Correction*

DNA polymerases contain two active sites, a polymerase site that catalyzes the reversible, template-directed elongation of DNA, and the exonuclease site, which catalyzes the hydrolysis of the 3′-terminal base. During processive synthesis, DNA replication occurs by the consecutive addition of bases without the intervening dissociation of the DNA, and the DNA can migrate between the polymerase site and the exonuclease site without dissociating from the enzyme (*12*). After the addition of each base pair, the enzyme–DNA complex partitions

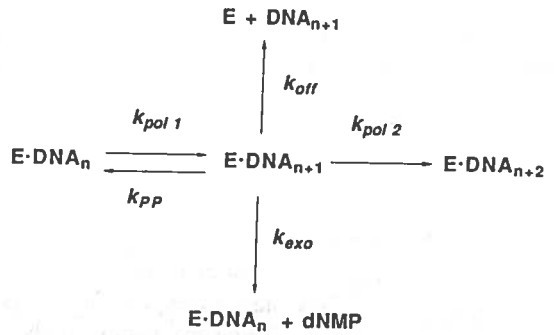

FIG. 13. DNA polymerase kinetic partitioning. The pathway shows the potential reactions during DNA replication: polymerization (k_{pol}), dissociation of the E–DNA complex (k_{off}), pyrophosphorolysis (k_{pp}), and exonuclease digestion of the 3′-terminal base (k_{exo}). Reproduced with permission from (*11*).

according to the kinetics of each of the optional pathways involving (1) continued polymerization, (2) reversal of polymerization by pyrophosphorolysis, (3) migration of the DNA to the exonuclease site, or (4) dissociation of the DNA from the enzyme, as illustrated in Fig. 13. This kinetic partitioning governs the fidelity and efficiency of DNA replication. After the incorporation of a correct base, the probability of continued incorporation is defined by the rate of polymerization divided by the sum of all other rates. According to the kinetic constants established for T7 DNA polymerase summarized in Table I (*10–12*), the probability of extension is quite high, with dissociation only once out of 1500 bases, and the exonuclease removes less than 0.1% of the correct bases. After an incorporation of the wrong base, the kinetic partitioning changes dramatically so that

TABLE I

DNA POLYMERASE KINETIC CONSTANTS[a]

Rate constant	Correct base (sec^{-1})	Incorrect base (sec^{-1})
$k_{pol\ 1}$	300	0.002
$k_{pol\ 2}$	300	0.013
k_{PP}	1	<0.0001
k_{off}	0.2	0.4
k_{exo}	0.2	2.8

[a] The kinetic constants governing the partitioning of the enzyme–DNA complex during normal polymerization (Correct) and with a mismatched base pair (Incorrect) are summarized (Ref). The rate constants are defined according to the pathway given in Fig. 13.

most of the mismatches are removed rather than extended, because the polymerase rate becomes very slow and the exonuclease rate is accelerated. This kinetic partitioning accounts for the high fidelity of replication catalyzed by T7 DNA polymerase and establishes the basis of the selectivity of the exonuclease in correcting errors.

G. Isotope and pH Effects

The effect of pH variation and isotope (or elemental) substitution on reaction kinetics has been used in the steady state to explore the roles of active site acid/base catalysts and to attempt to define the nature of the transition state (*8a*, *8b*, *58*). Each of these methods also depends on the extent to which the rate of the chemical reaction is rate limiting in the steady state. If some other step limits the rate of steady-state turnover, then changes in the rate of the chemical reaction will be obscured. Use of pH variation or isotope effects in transient kinetic experiments has been useful in a number of cases (*27*), especially where it has been possible to examine directly the rate of the chemical reaction at the enzyme active site. In these cases, the effect of pH or isotope substitution can be interpreted directly in terms of the effect on a single reaction.

The use of pH variation and isotope effects in transient kinetics can be illustrated with a recent study on dihydrofolate reductase. Analysis by steady-state methods had indicated an apparent pK_a of 8.5 that was assigned to an active site aspartate residue required to stabilize the protonated state of the substrate (*59*). In addition, it was shown that there was an isotope effect on substitution of NADPD (the deuterated analog) for NADPH at high pH but not at low pH, below the apparent pK_a. This somewhat puzzling finding was explained by transient-state kinetic analysis. Hydride transfer, the chemical reaction converting enzyme-bound NADPH and dihydrofolate to NAD^+ and tetrahydrofolate, was shown to occur at a rate of approximately 1000 sec^{-1} at low pH. The rate of reaction decreased with increasing pH with a pK_a of 6.5, a value more in line with expectations for an active site aspartate residue. As shown in Fig. 14, there was a threefold reduction in the rate of the chemical reaction with NADPD relative to NADPH. Thus direct measurement of the chemical reaction revealed the full isotope effect.

In the steady state, the release of products is rate limiting (14 sec^{-1}) and largely independent of pH. Figure 15 combines the pH dependence of the chemical reaction, product release, and steady-state turnover. At low pH, the chemical reaction is fast and product release limits the steady-state rate so there is no elemental effect observed in the steady state. As the pH is increased, there is a crossover in the identity of the rate-limiting step, so that at high pH the chemical reaction becomes rate limiting for steady-state turnover, leading to an observable isotope effect. The apparent pK_a of 8.5 in the steady state represents

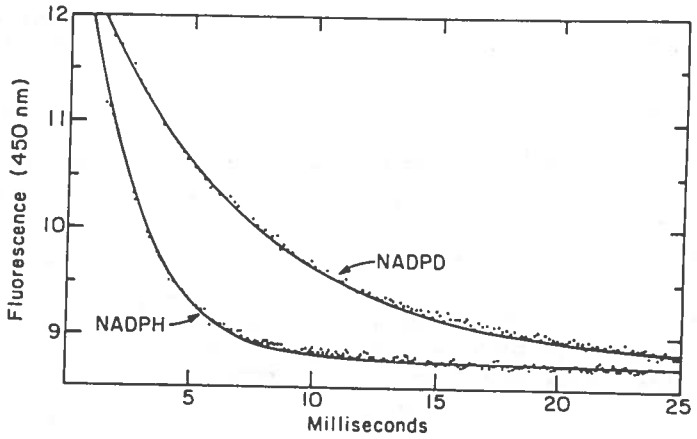

FIG. 14. Isotope effect on the rate of hydride transfer. The rate of hydride transfer to dihydrofolate catalyzed by dihydrofolate reductase (15 μM) was measured by fluorescence energy transfer, exciting the protein at 280 nm and observing emission by NADPH at 450 nm. The reaction with NADPH occurred at a rate of 450 sec^{-1}, followed by a linear phase at 12 sec^{-1}, as shown by the smooth line. The rate of the burst observed with NADPD, the deuterium analog, occurred at 150 sec^{-1}. Reproduced with permission from (*27*).

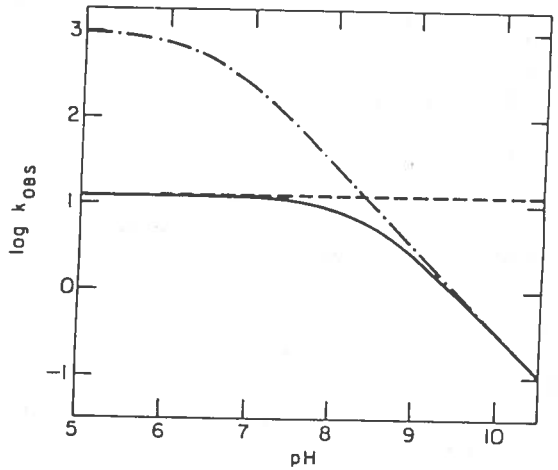

FIG. 15. The pH dependence of a reaction catalyzed by dihydrofolate reductase. The observed rate of hydride transfer (–·–) is compared with the rate of product release (---) and k_{cat}(—) on a log scale as a function of pH. The break in the rate of steady-state turnover at pH 8.5 is due to a change in the rate-limiting step from product release to hydride transfer. Reproduced with permission from (*27*).

the crossover point in switching from rate-limiting product release to rate-limiting chemistry.

This study has important lessons for enzyme kinetic analysis. The use of pH variation and examination of isotope effects can be a powerful combination to explore the chemistry of enzyme-catalyzed reactions and to dissect the contributions of individual reaction steps to the net steady-state turnover (*27*). Examination of the effects of pH on each step of the reaction pathway could resolve the contributions of ionizable groups toward ground-state binding energy and transition-state stabilization. The use of isotope effects by transient-state kinetic methods is more limited than in the steady state due to the errors involved in comparing two rate measurements. In the steady state, the ratio method has allowed isotope effects of less than 1% to be measured accurately (*8a, 58*). By transient-state kinetics, one would require at least a 10–20% change in rate to demonstrate a convincing difference between two rate measurements in most instances.

The use of a rate effect on the chemical reaction due to an elemental or isotope substitution has been used to test the extent to which an observed rate is a function of the chemical reaction. For example, in recent studies on DNA polymerase, use of dTTP(αS) in place of dTTP in a single-turnover experiment has provided evidence for a rate-limiting conformational change that precedes a much faster chemical reaction. Substitution of dTTP(αS) for dTTP should have resulted in a 100-fold reduction in the rate of reaction if chemistry were rate limiting (*10, 11*). The small (threefold) effect provided evidence to suggest that chemistry was not rate limiting, arguing indirectly for a protein conformational change involved in recognition of the correct base pair. Subsequent analysis has questioned the expectation of a 100-fold reduction in rate with the thio analog. The original estimation of a sulfur elemental effect by Benkovic and Shray (*60*) was based on the hydrolysis of phosphate triesters, while a recent study by Hershlag *et al.* (*61*) has indicated only a 4- to 10-fold sulfur effect for phosphate diesters. A more complete kinetic analysis of DNA polymerase mechanisms has substantiated the evidence for a conformational change following substrate binding, based on pulse-chase experiments (*10, 11*) and the observation of a protein fluorescence change by stopped-flow (*62*). Thus, the thio analog work may have given the right answer for the wrong reason.

VI. Methods of Data Fitting

The point of a transient kinetic experiment is to establish the reaction pathway by examination of the concentration dependence of the rate of reaction. It is the goal of proper data analysis to ferret out the best fit to the data to establish the reaction mechanism containing the minimal number of steps. I will describe two

approaches to data analysis: first, the conventional fitting of data to equations derived by integration of simple rate equations, and second, by computer simulation based on numerical integration of the equations describing the chemical reaction mechanism. In practice, both methods should be applied, with initial analysis by conventional data fitting, followed by refinement and convergence to a complete kinetic description of a reaction pathway by computer simulation. The standards set for this analysis now require the fitting of all data directly to a complete mechanism with no simplifying assumptions (*2, 3, 10–12*).

A. Conventional Data Fitting

The conventional data analysis involves the fitting of data to an equation describing the time dependence of the reaction, leading to the best estimates for the constants defining the equations. Analytical solutions to most simple reaction sequences can be obtained (*1, 5, 63*). Solutions of differential equations describing the series of first-order (or pseudo-first-order) reactions will always be a sum of exponential terms [Eq. (22)]. Thus for a single exponential, the fitting process provides the amplitude (A), the rate of reaction (λ), and the end point (C)

$$Y = Ae^{-\lambda t} + C$$

A proper fitting must include the minimization of the sum square error between the data and the calculated curve, allowing all three constants to float in converging to the optimal fit by nonlinear regression methods involving an iterative approach to the best fit. There are numerous reasons why the older methods involving linearization of the equations in a logarithmic form should not be used: (1) Logarithmic plots compress the most accurate data collected during the early stages of the reaction; (2) a value for the reaction endpoint must be assumed and errors in estimating the endpoint are propagated to alter the calculated rate; and (3) experimental values less than the endpoint cannot be included on a logarithmic plot, thus eliminating data collected late in the reaction. Modern computational methods based on nonlinear regression solve all of these problems by estimating the endpoint as a fitted parameter and by allowing the inclusion of data spanning six half-lives of the reaction (98% completion) even with a signal-to-noise ratio of 1.

For more complex kinetics, the data can be fit to an equation including two or more exponential terms. A double-exponential equation is defined by

$$Y = Ae^{-\lambda_1 t} + Be^{-\lambda_2 t} + C$$

The distinction between a single- and double-exponential fit is sometimes obvious, but in other cases, in which the difference in rates of reaction between the two phases is small (less than fourfold), it can be difficult to resolve the two rates. In these cases, the evaluation of the goodness of fit and the justification for including a second exponential term cannot be based solely on a reduction in

the sum square error. Visual evaluation of the fit is required, looking for systematic deviation of the fit from the data. The final fitting of the data should include computer simulation to ensure that the model predicts the observed concentration dependence of the rates and amplitudes of each phase and to justify the data fitting in terms of the reaction mechanism.

Presteady-state burst kinetics can be fit to an equation of the form

$$Y = A(1 - e^{-\lambda t}) + k_2 t$$

Fitting to this equation provides the rate and amplitude of the burst followed by the steady-state turnover rate during the linear phase. These rates and amplitudes can then be quantitatively evaluated in terms of the pathway and kinetic constants for the reaction as described above.

B. Computer Simulation of Complex Kinetics

Computer simulation has become increasingly important because it allows for analysis without any simplifying assumptions and includes amplitude information in the fitting process. Although any method can lead to errors in interpretation, computer simulation has been viewed with suspicion because the errors are made at the beginning of the analysis in writing the mechanism and choosing the best rate constants and it is difficult to document all of the logic that led to the convergence of the best fit to define the minimal mechanism. Nonetheless, the stringency with which a given model is fit to kinetic data is considerably higher by use of computer simulation because of the need to account for the concentration dependence of both the rate and amplitude of a reaction. Moreover, while there may be arguments as to whether a given mechanism can quantitatively account for a given set of kinetic data, there can be no such arguments with the proper use of computer simulation. The potential errors in conventional analysis of kinetic data arise from the simplifying assumptions that must be made to derive the appropriate equations; however, with computer simulation, there are no assumptions. The problem then becomes one of establishing a minimal kinetic scheme and quantitatively eliminating other possible mechanisms.

At first, the fitting of data to a reaction sequence may seem impossible, since not enough information is in hand to model the complete reaction. However, the fitting process should be based on identification of those rate constants that are defined by each experiment (*3, 39*). An initial fit to a given experiment to extract the critical rate constants can be based on a model with crude estimates for rate constants that do not affect greatly the fitting of that experiment. The results of fitting each experiment then provide the basis for fitting other experiments to define other rate constants. One can then return to the fitting of the first experiment based upon refined estimates of rate constants for each step in the pathway. With a bit of luck, enough experiments can be performed to constrain the fitting of the data to converge to a single solution. The computer program KINSIM has

now been extended to allow the fitting of reaction kinetics by nonlinear regression analysis based upon simulation (*64*). This analysis provides an estimate of the confidence limits on each kinetic parameter which allows the investigator to recognize when a given model is not sufficiently supported and constrained by the data.

The goal of a complete kinetic analysis is to define the rate and free energy change of each step in the reaction. Because the rates of each reaction in an enzymic pathway are comparable, the measurable events are kinetically linked and sometimes difficult to separate. Therefore, solution of an enzyme mechanism must include a fitting of all experiments to the complete model, including all steps in the pathway. Ideally one should measure each reaction in a sequence and then provide one additional measurement as a check for internal consistency. The two important checks on an enzyme reaction sequence are (1) measurement of the overall free energy change for the reaction in solution and (2) comparison of the predicted and measured steady-state kinetic constants.

VII. Résumé

In this chapter, I have attempted to provide a rationale for the design and interpretation of transient kinetic experiments to establish enzyme pathways by direct analysis of individual reaction steps. In many ways, transient kinetics are straightforward and experimental results can be understood in terms of simple principles derived from first-order kinetics. The application of these methods to enzyme kinetics was illustrated by a number of examples, and interested readers are encouraged to examine the original research publications to obtain a deeper understanding of the reaction kinetics. This is especially useful for those cases in which the kinetic data could be fit to a single, complete model, the most notable being EPSP synthase (*3*), DNA polymerase (*10–12*), and tryptophan synthase (*32*). The examples also served to strengthen the arguments in favor of computer simulation to analyze kinetic data. In many cases, the experiments could not have been interpreted quantitatively by any other means, but even in seemingly simple cases, the refinements resulting from computer simulation are significant. The most important danger in the interpretation of kinetic data stems from the tendency to include an additional reaction step to explain an unusual kinetic result, when often the new result could have been accounted for by a more simple model based on a deeper understanding of the subtleties of the kinetics. Thus, the overriding rule remains: Do not include a step in the mechanism unless there is direct evidence for it or the fitting of the data absolutely requires it. Although computer simulation has been viewed with some caution because it is perhaps too easy to include an unnecessary step, it should also be recognized that computer simulation also permits the quantitative evaluation of the most simple models in fitting kinetic data.

The application of transient kinetic methods to the solution of enzyme mechanisms has increased dramatically due to recent advances in instrumentation and in the overexpression and purification of new enzymes. Transient kinetics are becoming the method of choice for evaluation of site-directed enzyme mutants and for detailed questions regarding the relationships between protein structure and observable function. In conjunction with advances in methods of structural and genetic analyses, transient-state kinetic analysis forms the basis for what might be called the "new enzymology."

Acknowledgments

I would like to thank Karen S. Anderson (Yale University, New Haven, CT) for her careful reading of this manuscript.

References

1. Johnson, K. A. (1986). *In* "Methods in Enzymology" (R. B. Vallee, ed.), Vol. 134, pp. 677–705. Academic Press, New York.
2. Barshop, B. A., Wrenn, R. F., and Frieden, C. (1983). *Anal. Biol.* **130,** 134.
3. Anderson, K. S., Sikorski, J. A., and Johnson, K. A. (1988). *Biochemistry* **27,** 7395.
4. Hammes, G. (1970). "The Enzymes," 3rd Ed., Vol. 2, pp. 65–114.
5. Fersht, A. R. (1985). "Enzyme Structure and Mechanism," 2nd Ed., Freeman, San Francisco, California.
6. Cleland, W. W. (1970). "The Enzymes," 3rd Ed., Vol. 2, pp. 1–64.
7. Cleland, W. W. (1991). "The Enzymes," 3rd Ed., Vol. 19, pp. 99–158.
8. Johnson, K. A., and Benkovic, S. J. (1991). "The Enzymes," 3rd Ed., Vol. 19, pp. 159–211.

8a. Cleland, W. W. (1982). *In* "Methods in Enzymology" (D. L. Purich, ed.), Vol. 87, pp. 625–626. Academic Press, New York.

8b. Cleland, W. W. (1982). *In* "Methods in Enzymology" (D. L. Purich, ed.), Vol. 87, pp. 390–405. Academic Press, New York.

9. Fersht, A. R. (1987). *Biochemistry* **26,** 8031.
10. Patel, S. S., Wong, I., and Johnson, K. A. (1991). *Biochemistry* **30,** 511.
11. Wong, I., Patel, S. S., and Johnson, K. A. (1991). *Biochemistry* **30,** 526.
12. Donlin, M. J., Patel, S. S., and Johnson, K. A. (1991). *Biochemistry* **30,** 538.
13. Del Rosario, E. J., and Hammes, G. G. (1971). *Biochemistry* **10,** 716.
14. Hurst, J. K., and Hammes, G. G. (1969). *Biochemistry* **8,** 1083.
15. Anderson, K. S., Sikorski, J. A., Benesi, A. J., and Johnson, K. A. (1988). *J. Am. Chem. Soc.* **110,** 6577.
16. Anderson, K. S., Sammons, R. D., Sikorski, J. A., Leo, G. E., Benesi, A. J., and Johnson, K. A. (1990). *Biochemistry* **29,** 1460.
17. Barlow, P. N., Appleyard, R. J., Wilson, B. J. O., and Evans, J. N. S. (1989). *Biochemistry* **28,** 7985.
18. Albery, W. J., and Knowles, J. R. (1976). *Biochemistry* **15,** 5631.
19. Burbaum, J. J., Raines, R. T., Albery, W. J., and Knowles, J. R. (1989). *Biochemistry* **28,** 9293.
20. Burbaum, J. J., and Knowles, J. R. (1989). *Biochemistry* **28,** 9306.

21. Andrawis, A., Johnson, K. A., and Tien, M. (1987). *J. Biol. Chem.* **263,** 1195–1198.
22. Cai, D., and Tien, M. (1990 *Biochemistry* **29,** 2085.
23. Drewe, W. F., and Dunn, M. F. (1985). *Biochemistry* **24,** 3977.
24. Drewe, W. F., and Dunn, M. F. (1986). *Biochemistry* **25,** 2494.
25. Lane, A., and Kirschner, K. (1983a). *Eur. J. Biochem.* **129,** 561.
26. Lane, A., and Kirschner, K. (1983b). *J. Biochem. (Tokyo)* **129,** 571.
27. Fierke, C. A., Johnson, K. A., and Benkovic, S. J. (1987). *Biochemistry* **26,** 4085.
28. Johnson, K. A., and Taylor, E. W. (1978). *Biochemistry* **17,** 3432.
29. Holbrook, J. J., Liljas, A., Steindel, S. J., and Rossmann, M. G. (1975). "The Enzymes," 3rd Ed., Vol. 2, pp. 191–268.
30. Rosenfeld, S. S., and Taylor, E. W. (1984). *J. Biol. Chem.* **259,** 11920.

30a. Woodward, S. K. A., Eccleston, J. F., and Geeves, M. A. (1991). *Biochemistry* **30,** 422.

31. Anderson, K. S., and Johnson, K. A. (1990). *Chem. Rev.* **90,** 1131.
32. Anderson, K. S., Miles, E. W., and Johnson, K. A. (1991). *J. Biol. Chem.* **266,** 8020.
33. Anderson, K. S., Sikorski, J. A., and Johnson, K. A. (1988). *Biochemistry* **27,** 1604.
34. Wells, T. N. C., and Fersht, A. R. (1986). *Biochemistry* **25,** 1881.
35. Fersht, A. R., Leatherbarrow, R. J., and Wells, T. N. C. (1987). *Biochemistry* **26,** 6030.
36. Fersht, A. R., Knill-Jones, J. W., Bedouelle, H., and Winter, G. (1988). *Biochemistry* **27,** 1581.
37. Johnson, K. A. (1985). *Annu. Rev. Biophys. Biophys. Chem.* **14,** 161.
38. Gutfreund, H. (1972). "Enzymes: Physical Principles." Wiley (Interscience), New York.
39. Johnson, K. A. (1983). *J. Biol. Chem.* **258,** 13825.
40. Remington, S., Wiegand, G., and Huber, R. (1982). *J. Mol. Biol.* **158,** 111.
41. Hackney, D. D., Malik, A. S., and Wright, K. W. (1989). *J. Biol. Chem.* **264,** 15943.
42. Hartley, B. S., and Kilby, B. A. (1954). *Biochem. J.* **56,** 288.
43. Gutfreund, H., and Hammond, B. R. (1959). *Biochem. J.* **59,** 526.
44. Anderson, K. S., and Johnson, K. A. (1990). *J. Biol. Chem.* **265,** 5567.
45. Srere, P. A. (1987). *Annu. Rev. Biochem.* **56,** 89.
46. Welch, G. R. (1977). *Prog. Biophys. Mol. Biol.* **32,** 103.
47. Keleti, T., and Ovadi, J. (1988). *Curr. Top. Cell. Regul.* p. 1.
48. Weber, J. P., and Bernhard, S. A. (1982). *Biochemistry* **21,** 4189.
49. Srivastava, D. K., and Bernhard, S. A. (1985). *Biochemistry* **24,** 623.
50. Srivastava, D., and Bernhard, S. A. (1986). *Science* **234,** 1081.
51. Chock, B. P., and Gutfreund, H. (1988). *Proc. Natl. Acad. Sci. U.S.A.* **85,** 8870.
52. Kvassman, J., and Petterson, G. (1989). *Eur. J. Biochem.* **186,** 261.
53. Kvassman, J., and Petterson, G. (1989). *Eur. J. Biochem.* **186,** 265.
54. Srivastava, D. K., and Bernhard, S. A. (1987). *Biochemistry* **26,** 1240.
55. Hyde, C. C., Ahmed, S. A., Padlan, E. A., Miles, E. W., and Davies, D. R. (1988). *J. Biol. Chem.* **263,** 17857.
56. Dunn, M. F., Aguilar, V., Brzovic, P., Drewe, W. F., Houben, K. F., Leja, C. A., and Roy, M. (1990). *Biochemistry* **29,** 8598.
57. Houben, K. F., and Dunn, M. F. (1990). *Biochemistry* **29,** 2421.
58. Cook, P. F., and Cleland, W. W. (1981). *Biochemistry* **20,** 1797.
59. Stone, S., and Morrison, J. F. (1984). *Biochemistry* **23,** 2757.
60. Benkovic, S. J., and Schray, K. (1973). "The Enzymes," 3rd Ed., Vol. 8, pp. 201–236.
61. Hershlag, D., Piccirilli, J. A., and Cech, T. R. (1991). *Biochemistry* **30,** 4844.
62. Patel, S., Wong, I., and Johnson, K. A. (1991). Unpublished results.
63. Capellos, C., Bielski, B. H. J. (1972). "Kinetic Systems: Mathematical Description of Chemical Kinetics in Solution" (Wiley-Interscience).
64. Zimmerle, C. J., and Frieden, C. (1989). *Biochemistry J.* **258,** 381–387.